A Dissertation for the Degree of Doctor of Philosophy

Amelioration Mechanisms of Neurodegenerative Process in Niemann-Pick Disease type C1

니만-픽크 C1 형 질환에서

신경 퇴행성 변화의 완화 기전

By

Yoojin Seo

February 2015

Department of Veterinary Medicine,

Graduate School of Seoul National University

ABSTRACT

Amelioration Mechanisms of Neurodegenerative Process in Niemann-Pick Disease type C1

Yoojin Seo

Department of Veterinary Medicine,
Graduate School of Seoul National University

Supervisor: Kyung-Sun Kang, D.V.M., Ph.D.

Niemann-Pick disease type C (NPC) is an incurable neurodegenerative disorder with disrupted lipid trafficking and it is characterized by progressive neurological deterioration leading to premature death. Therefore, the primary goal of my study is to understand the underlying mechanisms of the neuropathology and to suggest the novel treatment strategies for this incurable disease. In this purpose, I evaluated the therapeutic potential of (1) human umbilical cord blood-derived mesenchymal stem cells (hUCB-

MSCs) and (2) microglial inhibitor for NPC management using NPC1 mice model.

In the first study, I hypothesized that hUCB-MSCs have multifunctional abilities to improve the neurological symptoms of NPC1, the main subtype of NPC. To test this hypothesis, hUCB-MSCs were directly transplanted into the hippocampus of NPC1 mice model at the early asymptomatic stage. This transplantation resulted in improvement of motor function in the Rota-rod test and recovery of impaired cholesterol homeostasis via stimulating the cholesterol efflux system of the NPC1 mice. In the hippocampus, hUCB-MSCs increased the neuronal survival and proliferation while some of treated cells underwent *in vivo* transdifferentiation into functional neurons with electrophysiological activity in whole-cell patch clamping. Further, hUCB-MSCs reduced Purkinje neuronal loss, the hallmark of NPC1 neuropathic signs, by suppressing inflammatory- and apoptotic signaling in the cerebellum. I found that neuroprotective actions of hUCB-MSCs were resulted from enhanced cell-survival signals including PI3K/AKT- and JAK2/STAT3 pathways as well as from corrected expression levels of GABA/glutamate transporters followed by decreased excitotoxicity in the NPC1-affected brain.

In the second study, I focused on the pathology of NPC1-related olfactory bulb (OB), the least studied area in the NPC1-affected brain, to provide more novel findings in the field of NPC1. NPC1 mutants at 7 weeks of age showed a distinct olfactory impairment in the buried food test when compared with age-matched WT controls. I found the marked loss of olfactory sensory neurons and dopaminergic periglomerular neurons within the NPC1-OB, suggesting that NPC1 dysfunction impairs the integrity of the olfactory structure. The gradual denervation of olfactory sensory neurons in NPC1

mice led to a reduction in the neuroblast population within the OB; however, the total number of proliferating cells was found to be increased because microglia extensively accumulated in the NPC1-OB along with pro-inflammatory cytokines, including IL-1β and TNF-α, as the disease progresses. Therefore, then I evaluated the effects of the anti-inflammatory drug CsA on olfactory dysfunction in NPC1 mice to investigate the possible role of microgliosis on olfaction. My experiments revealed that treatment with CsA prevented reactive microgliosis, restored the proliferative capacity of neuroblasts and increased the number of newly generated OB interneurons. In addition, NPC mice displayed an improvement in overall performance in the buried food test after the chronic administration of CsA.

Taken together, these findings imply that (1) direct transplantation of hUCB-MSCs into the NPC1-affected mouse brain reduces neuropathies including cholesterol imbalance and neural death both in the cerebrum and cerebellum and (2) microglial inhibition using immunosuppressive agent attenuates of olfactory impairment in NPC1 mice via the regulation of neuronal turnover in the OB. Therefore, my study suggests novel therapeutic approaches for the amelioration of neurodegenerative symptoms in NPC1.

Keywords : Niemann-Pick disease Type C1; Neurodegeneration; Neuroprotection; Human umbilical cord blood mesenchymal stem cells; Stem cell therapy; Microglia; Immunosuppressant; Cyclosporin A

Student number: 2009-21625

TABLE OF CONTENTS

LIST OF ABBREVIATION

ABCA1	**ATP-binding membrane cassette transporter type A1**
ABCG5	**ATP-binding membrane cassette transporter type G5**
AD	**Alzheimer`s disease**
ALS	**Amyotrophic lateral sclerosis**
AP5	**2-Amino-5-phosphopentanoic acid**
Aβ	**Amyloid-β**
BAX	**Bcl-2 associated X-protein**
BrdU	**5-Bromo-2'-deoxyuridine**
CBD	**Calbindin**
COX2	**Cyclooxygenase2**
CNQX	**6-Cyano-7-nitroquinoxalin-2, 3-dione**
CsA	**Cyclosporin A**
DAPI	**4', 6-Diamidino-2-phenylindole, dihydrochloride**
DCX	**Doublecortin**
DG	**Dentate gyrus**
EAAT2	**Excitatory amino acid transporter 2**
EAAT3	**Excitatory amino acid transporter 3**

ER	**Endoplasmic reticulum**
FBS	**Fetal bovine serum**
GAD65	**Glutamic acid decarboxylase 65**
GAPDH	**Glyceraldehyde 3-phosphate dehydrogenase**
GAT1	**GABA transporter 1**
GC	**Granule cells**
GCL	**Granule cell layer**
GFAP	**Glial fibrillary acidic protein**
GL	**Glomerular layer**
GSK3β	**Glycogen synthase kinase 3β**
HMGR	**3-Hydroxy-3-methylglutaryl coenzyme A reductase**
hUCB	**Human umbilical cord blood**
HuMi	**Human mitochondria**
IL	**Interleukin**
iNOS	**Inducible nitric oxide synthase**
JAK2	**Janus kinase 2**
LE/L	**Late endosome and lysosome**
LXR	**Liver X-receptor**
MAP2	**Microtubule associated protein 2**
MSC	**Mesenchymal stem cell**

NeuN	**Neuronal nuclei**
NPC	**Niemann-Pick disease type C**
NSC	**Neural stem cell**
OB	**Olfactory bulb**
OE	**Olfactory epithelium**
OMP	**Olfactory marker protein**
OSN	**Olfactory sensory neurons**
PBS	**Phosphate buffered saline**
PD	**Parkinson's disease**
PGC	**Periglomerular cell**
PI3K	**Phosphoinositide 3 kinase**
STAT	**Signal transducers and activators of transcription protein**
SVZ	**Subventricular zone**
TH	**Tyrosine hydroxylase**
TNF-α	**Tumor necrosis factor-α**
TTX	**Tetrodotoxin**
WT	**Wild-type**

LIST OF FIGURES & TABLE

LITERATURE REVIEW

Niemann-Pick disease type C1 (NPC1)

Niemann-Pick disease type C (NPC) is an autosomal recessive, fatal disease found in approximately one among 120,000 live births (Vanier, 2010). The majority (~95%) of NPC cases are caused by genetic mutations in the NPC1 gene, referred to as type C1 (NPC1), while remained 5% of cases are originated from the NPC2 gene mutation, referred to as type C2 (NPC2) (Pentchev et al., 1985). The main characteristic of NPC1- and NPC2 affected cells is an extensive accumulation of cholesterol and other lipids within the late endosome and lysosome (LE/L) due to impaired intracellular cholesterol trafficking (Tang et al., 2010).

Cholesterol is an essential component of cell membranes as well as a primary source of steroid hormones, vitamins and other lipid complex (Hanukoglu, 1992). In the periphery, cholesterol can be produced through de novo biosynthesis pathway or exogenous cholesterol from dietary sources binds to low-density lipoproteins (LDLs) and LDL-cholesteryl ester complex is uptake into the cells via endocytosis (Ye and DeBose-Boyd, 2011). On the other hand, since plasma lipoproteins cannot enter into the brain due to the presence of blood-brain barrier, adequate cholesterol supply of the normal brain is entirely dependent on the cholesterol biosynthesis and glial cells are known to be the primary provider of neuronal cholesterol (Pfrieger, 2003). Once cholesterol moves inside

the cytosol, it is transported to the LE/L and cholesterol is released from LDL complex (periphery) or from ApoE complex (brain) as an unesterified form by lysosomal acid lipase-mediated hydrolysis. Then unesterified cholesterol exits the LE/L to enter the endoplasmic reticulum (ER), where re-esterification of cholesterol and assembly of LDL occurs or to reach the plasma membrane for redistribution (Ikonen, 2008). It is widely accepted that this last step, transportation of cholesterol from LE/L to the next organelles, is severely impaired in NPC-affected cells. Based on the fact that clinical manifestations of NPC1 and NPC2 are almost identical, both NPC1 and NPC2 genes seem to be associated with cholesterol egress process in the LE/L, although the exact mechanism of NPC1/2 mediated cholesterol trafficking has not been clearly elucidated. In the recent proposed model, soluble protein NPC2 binds and delivers free cholesterols to trans-membranous protein NPC1 that exports cholesterols outside the LE/L (Fig. 1) (Kwon et al., 2009; Rosenbaum and Maxfield, 2011; Subramanian and Balch, 2008). Thus, dysfunction of NPC1 or NPC2 proteins leads to massive accumulation of unesterified cholesterol within the LE/L, while ER and plasma membrane suffer from the lack of cholesterol at the same time. Because ER functions as the principal surveillance of the cholesterol homeostasis, false signal of cholesterol depletion in ER results in up-regulation of cholesterol biosynthesis, which causes a vicious cycle of cholesterol imbalance in NPC status (Karten et al., 2009; Peake and Vance, 2010). Besides unesterified cholesterol, a variety of other lipids, including sphingosine, sphingomyelin, glycosphingolipids (mainly the gangliosides GM2 and GM3) also accumulate in the LE/L of NPC-deficient cells (Vance, 2006). Among those various lipids, pointing out the one

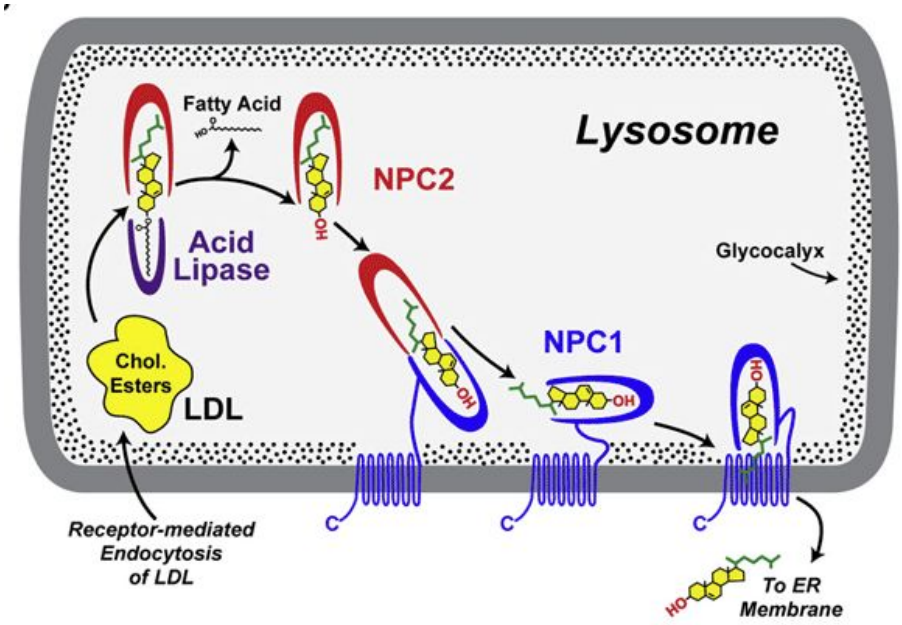

Figure 1. Process of intracellular trafficking model of cholesterol and Related NPC1/2 function.

Cholesterol esters in the form of LDL bind to the LDL receptor and are endocytosed and delivered to the LE/L then released from LDL interact with a complex of NPC2 and acid lipase. Fatty acid chains are removed from the cholesterol esters by acid lipase to yield NPC2-cholesterol complexes. Next, cholesterol is then transferred to the N-terminal domain of NPC1. Finally, cholesterol is exported from the endo-lysosomes by an unknown NPC1-mediated mechanism (Suggested model by Brown and Goldstein) (Kwon et al., 2009).

that initiates NPC pathology is still under debate but cholesterol is thought to be playing the primary roles because it is the only lipid that can directly interact with NPC1/2 via their binding domain (Kwon et al., 2009; Xu et al., 2007). In addition, staining results of NPC animal model samples with an unesterified cholesterol binding agent filipin show that cholesterol already accumulates from non-symptomatic stage and artificially induced cholesterol accumulation can lead to glycosphingolipid sequestration in the LE/L, while depletion of cholesterol using chemicals prevent other lipid storage (Puri et al., 1999). Thus, regulation of cholesterol accumulation and distribution is considered as the key therapeutic strategy in NPC management.

Although the onset point and symptoms of NPC are considerably various between affected individuals, most of the patients die before their 20s (Vanier, 2010). Because NPC1/2 proteins are ubiquitously expressed within the mammalian cells, NPC is considered as a neurovisceral disorder and liver, spleen, lung and brain are the most involved organs. In typical patients, hepatosplenomegaly and jaundice develop followed by the neurological manifestation such as cerebellar ataxia, dysarthria, dysphagia, and progressive dementia, and vertical supranuclear gaze palsy. Importantly, the presence of neurological symptoms is regarded as the most decisive factor in determining the prognosis of NPC because it is ultimately responsible for the death of most patients (Fraile et al., 2010; Heron and Ogier, 2010). Considering that delayed development of neurological symptoms is largely related to the longer survival of patients (Fig. 2) (Vanier, 2010; de Baulny, 2010), majority of attempts to treat NPC are focused on the regulation/amelioration of neuropathology in NPC status.

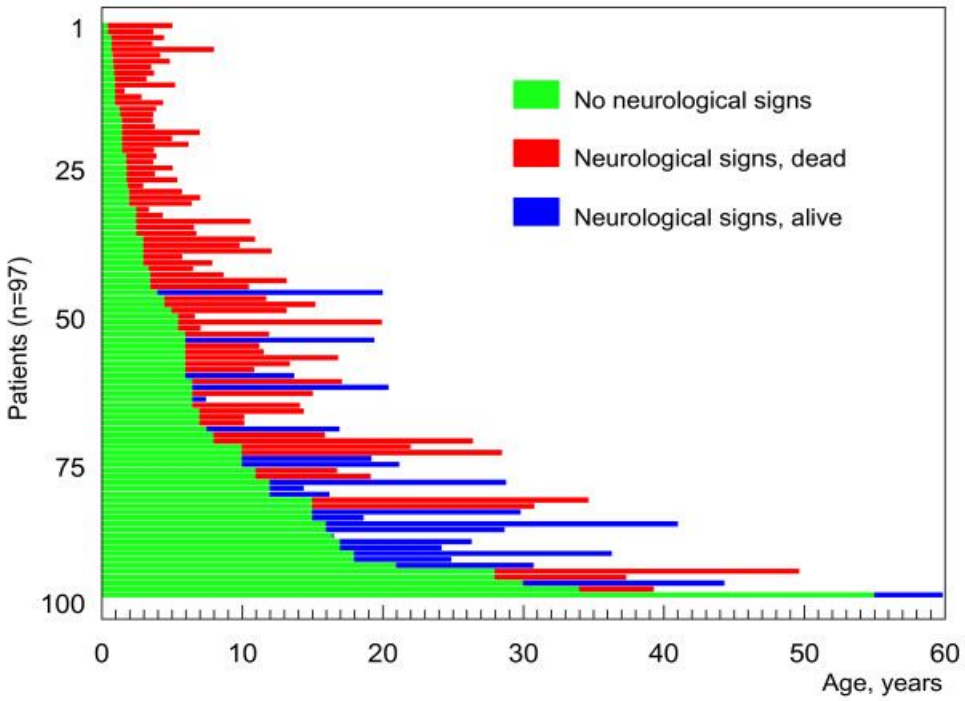

Figure 2. Age of onset of neurological disease vs lifespan of 97 NPC-affected patients. Each horizontal bar depicts one patient. The green color indicates the period during which the patient did not present neurological symptoms, irrespective of the presence or absence of preexisting systemic disease (Vanier, 2010).

In the brain, the progressive pathological features of NPC are found in the thalamus, cortex and hippocampus as well as in the cerebellum, the most obviously damaged area (Paul et al., 2004). Since cholesterol-rich myelin (contains 80% of total brain cholesterol) is significantly reduced due to the massive death of oligodendrocytes in the NPC-affected brain, typical accumulation of cholesterol is not observed in the brain; however, NPC-derived neurons show abnormal cholesterol distribution in their axons and fail to react properly to the brain-derived neurotrophic factor signaling (Henderson et al., 2000). Also, selective loss of Purkinje neurons in the cerebellum and other regional neurons is the hallmark of NPC-related neurodegeneration (Sarna et al., 2003). Several experiments with genetically engineered mice showing that Purkinje cell-specific loss of NPC1 gene in wild type mouse is sufficient to reproduce the death of Purkinje neurons as observed in typical NPC1-affected cerebellum (Elrick et al., 2010b; Yu et al., 2011), while Purkinje cell-specific recovery of NPC1 gene in NPC1 mouse can protect Purkinje cell population (Lopez et al., 2011), provide evidence of autonomous neuronal damage in NPC. Interestingly, Purkinje neuronal pathology might not be responsible for the weight loss and premature death ultimately but rather the death of thalamic regional neurons seems to have a close connection with detrimental progress of NPC (Elrick et al., 2010; Lopez et al., 2011). It is suggested that apoptosis and autophagy in the NPC affected brain contribute to the independent death of neurons. Compare to WT counterpart, enhanced expression level of caspase-3 and tumor necrosis factor-α associated signal is well observed accordance with increased number of TUNEL positive cells in the NPC mice brain (Wu et al., 2005). In addition, since NPC1/2 proteins are also related to lysosomal

fusion and fission as well as vesicle transport, autophagic process is largely impaired in NPC status which can lead to Purkinje cell loss in the brain (Sarkar et al., 2013). Even though neuron is the primary target cell in the NPC affected brain, growing evidence is showing that non-neural cells including astrocyte, microglia and oligodendrocyte also have roles in neurodegenerative process in NPC in response to neuron-associated pathologic changes (Erickson, 2013); NPC1 deficiency in oligodendrocyte population impairs myelin production, causing ineffective neuronal communication (Yu and Lieberman, 2013) and decreased neurosteroid secretion by NPC1-null astrocytes results in neurite malformation and neural death (Chen et al., 2007). Also, NPC1 deficient microglia produce extensive amount of cytotoxic cytokines such as TNF-α and IL-1β and microgliosis develops earlier than any other sign of neuronal loss in the NPC1 mouse brain (German et al., 2002). Therefore, more studies considering not only neurons but also other glial cells have to be done to depict the overall neurodegenerative process of NPC.

To date, no FDA-approved therapy is available for NPC and present therapeutic approaches are mainly focused on symptomatic control. The main scheme of NPC therapy is to reduce or prevent cholesterol and other lipids sequestration. As neuropathy development is the most important aspect of NPC to determine the prognosis, drugs or therapeutic methods must enter into the brain regardless of blood-brain barrier. In this context, 2-HP-β-cyclodextrin is suggested as a potential therapeutic agent for NPC according to its ability to bind and remove cholesterol and lipid from cells (Abi-Mosleh et al., 2009; Rosenbaum et al., 2010; Walkley et al., 2010). A glicosphigolipid

biosynthesis inhibitor Miglustat also provides similar beneficial effects on NPC neurological symptoms (Wraith et al., 2010). The therapeutic usage of both drugs is under clinical trial phase I. In addition, research is continuing to identify potential treatments that could either slow or stop the progression of the disease using animal models.

Application of Stem Cell therapy in the field of Neurodegenerative Disease

It was strongly believed that cells in the brain, especially neurons, have no proliferative capacity in postnatal life. This dogma was broken by finding of newly generated neural stem/progenitor cells in the subventricular zone of the lateral ventricle wall and dentate gyrus of the hippocampus (Ming and Song, 2011); however, it is still widely accepted that brain is one of the least active organs in the context of regenerative activity. Various stimuli such as mild inflammation can stimulate neurogenic center residing- or locally existing neural stem/precursor cells to proliferate and differentiate into mature cells but prolonged presence of neurotoxic signals as found in ageing and neurodegenerative process impedes neurogenesis and overwhelms innate regenerative capacity, leading to irreversible brain damage (Grote and Hannan, 2007; Winner et al., 2011). Therefore, not only removal of pathologic factor such as amyloid β in Alzheimer`s disease, but also replacement of damaged neurons or amelioration of microenvironment for neurogenesis is regarded as an important goal in the field of neurodegenerative disease therapeutics. Thus, application of stem cells in neurodegenerative situation has attracted great attention.

As stem cells have potential to differentiate into other mature cells according to their inherent nature, they have been used to treat a variety of disorders in terms of regenerative medicine and tissue engineering. For the stem cell application to brain-associated disorder, neural stem cells (NSCs) would be the best stem cell type but there are lots of restrictions to obtain and maintain them. Embryonic stem cells (ES) have potential to differentiate into neural lineage but well-known ethical problems and development of differentiation technique that evades teratoma formation limit usage of ES. In this context, stem cell based therapeutic attempts have used mesenchymal stem cells (MSCs) because MSCs are abundantly distributed entire body and easier to collect when compared to NSCs and ES. Moreover, adult-derived MSCs can be used in autologous therapies, in which ethical and immune-rejection problems would be eliminated.

MSCs are isolated from mesoderm-originated tissue including bone marrow, adipose tissue, dental pulp, amniotic fluid and umbilical cord blood (Beyer Nardi and da Silva Meirelles, 2006). MSCs primarily differentiate into mesodermal lineage cells including osteocyte, adipocyte and chondrocyte. It is also reported that they can undergo transdifferentiation into other cell lineages such as neurons upon manipulation of differentiation condition (Jiang et al., 2002; Phinney and Prockop, 2007), although the acquisition of proper function of transdifferentiated cells is under debate. In addition, logical basis of naïve MSC application in neurodegenerative disease is not only based on their multipotency for replenishment of lost neurons but also on their protective support to reduce neural damage in the pathological condition (Fig. 3) (Eckert et al., 2013; Joyce

et al., 2010; Tanna and Sachan, 2014). Upon transplantation, MSCs provide variety of paracrine effects through secretion of multiple growth factors and immune-modulatory factors. MSC-derived neurotrophic factors such as brain derived neurotrophic factor, glia derived neurotrophic factor, Insulin like growth factor 1 and neurotrophin 3/4 stimulate endogenous stem cell proliferation and increase neurite regeneration in various neuropathological condition (Crigler et al., 2006). MSCs also reduce the severity of neuroinflammation via direct suppression of immune cells with nitric oxide, prostaglandin-E2, transforming growth factor-β1 and IL-10 (Ren et al., 2008). These advantages of MSCs contribute to positive outcomes in experimental analysis of therapeutic potential of MSCs in various neurodegenerative conditions such as Parkinson`s disease (Bouchez et al., 2008; Sadan et al., 2009), multiple sclerosis (Burman et al., 2014; de Paula et al., 2015) and Amyotrophic lateral sclerosis (Vercelli et al., 2008; Zhao et al., 2007). The beneficial effect of MSCs in NPC1 status has been also challenged (Lee et al., 2010; Seo et al., 2011); transplantation of bone marrow- and adipose tissue derived MSCs as well as umbilical cord blood derived MSCs provides protection of Purkinje cell population, recovers impaired neuronal synaptic activity, alleviates excessive neuroinflammation and reduces cholesterol/lipid accumulation. Clinically, MSC-treated NPC1 mice show a meaningful recovery of motor function in most cases, suggesting MSC transplantation as a potential NPC therapeutic approach.

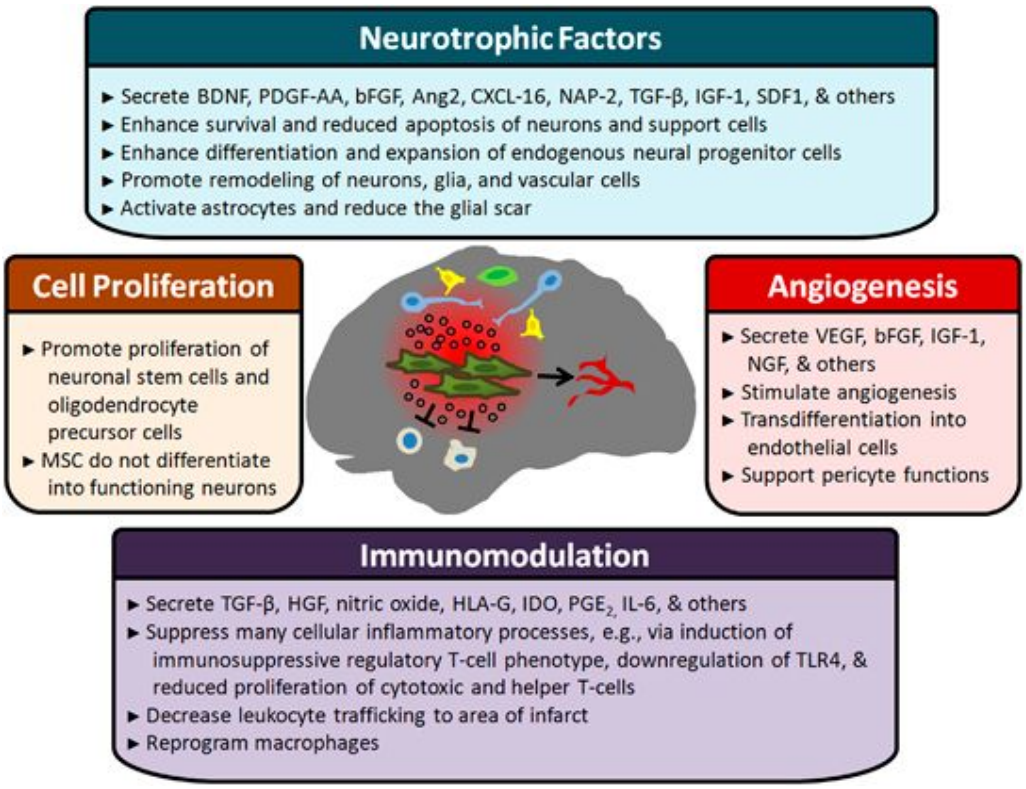

Figure 3. Overview of proposed mechanisms of mesenchymal stem cells (MSC)-based neurological disorder therapies.

Important potential mechanisms mediating MSC action in stroke include secretion of neurotrophic factors promotion of angiogenesis and modulation of immune responses. Note that some of the factors secreted by MSC may have multifactorial roles, i.e., affect multiple pathways. Cell replacement is no longer thought to play a major role in the therapeutic effects of MSC in stroke; although transplanted MSC may express markers of neuronal lineage, there is no evidence that they are functional. In the figure, MSC are olive colored, neurons are blue, glial cells are yellow, neural progenitor cells are green, and immune cells are tan (Eckert et al., 2013).

There are several essential points to be solved before clinical application of MSC therapy in neurodegenerative disease. (Prockop, 2009) First, appropriate cell delivery route must be determined. Regarding the presence of blood brain barrier, direct cell injection into the brain lesion would be the most certain method but it could be too invasive and dangerous. On the contrary, intravenous delivery of cells is widely used in clinical trials but it could not guarantee the entrance of cells into intended target site in the brain. Thus, cell tracking method is needed to evaluate transplanted cell distribution and excretion. In addition, transplanted MSCs can be rejected immediately because brain has a segregated immune system from periphery. Finally, as the most of benefits of cell therapy seem to be originated from paracrine effect, additional efforts to increase treated cell survival is necessary to maximize the overall effect of MSC delivery.

Contribution of Microglial in the Neurodegenerative Process

Central nervous system (CNS) consists of neurons and supportive glial cells including oligodendrocytes, astrocytes and microglia. Unlike other cells derived from ectodermal lineage, microglia are known to be originated from mesodermal hematopoietic lineage and their primitive progenitors in the yolk sac migrate into the developing brain during early embryogenesis (Ginhoux et al., 2013). Microglia perform constant surveillance activity, thereby being considered as the resident macrophages in the CNS and maintain their population via consistent local proliferation throughout life time (Ajami et al., 2007).

In the normal mature CNS, majority of microglia are under steady state with ramified morphology, so called 'resting microglia'. Besides their immune surveillance role, resting microglia contribute to many biological processes in the CNS including neurogenesis (Tremblay et al., 2011). It has been well described that microglia participate in arrangement of the appropriate neural circuits by removing cell debris during the embryonic period and early postnatal life (Ashwell, 1991). Even in resting state, microglia residing nearby neurogenic center such as olfactory bulb and subgranular zone perform phagocytosis of apoptotic cells during neurogenesis (Fig. 4) (Sierra et al., 2010; Sierra et al., 2014; Cunningham et al., 2013).

When microglia become activated in response to various environmental stimuli, they expand their population (microgliosis) as well as transform into amoeboid like morphology with increased secretion of cytokines and inflammatory mediators. Indeed, almost every neuropathic condition is accompanied to extensive microglial activation with profound microgliosis (Perry et al., 2010). Activated states of microglia are often divided into two status as classical activation (M1) and alternative activation (M2) according to the activating factors (M1: LPS and IFNγ; M2:IL-4 and IL-13), expressed cell specific markers (M1: CD86; M2: CD206) and their main biological functions (M1: production of pro-inflammatory molecules; M2: enhanced phagocytosis), although this M1-M2 microglia classification has a weak point mainly stem from the fact that it overlooks the plasticity and complexity of microglial nature and there is no actual boundary found between their phenotypes (Mosser and Edwards, 2008; Perry et al., 2010). Microglia can provide both beneficial and detrimental effects on

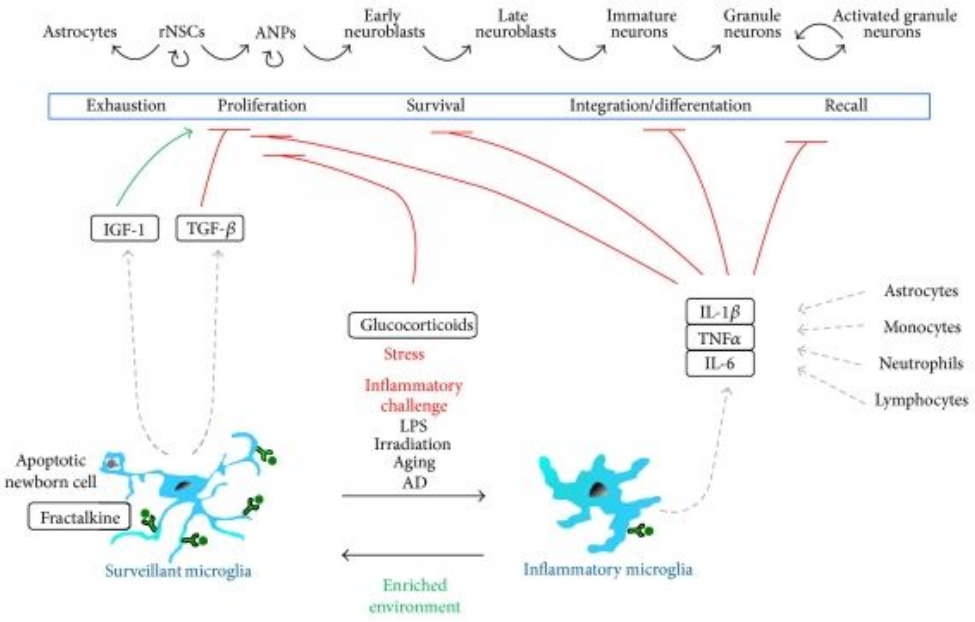

Figure 4. The role of microglia on the adult hippocampal neurogenic cascade.

During physiological conditions, surveillant microglia effectively phagocytose the excess of apoptotic newborn cells and may release antineurogenic factors such as TGF. This anti-inflammatory state is maintained by neuronal fractalkine. Enriched environment drives microglia towards a phenotype supportive of neurogenesis, via the production of IGF-1. In contrast, inflammatory challenge triggered by LPS, irradiation, aging, or AD induces the production of proinflammatory cytokines such as IL-1, TNF, and IL-6 by microglia as well as resident astrocytes and infiltrating monocytes, neutrophils, and lymphocytes. These cytokines have profound detrimental effects on adult neurogenesis by reducing the proliferation, survival, integration, and differentiation of the newborn neurons and decreasing their recall during learning and memory paradigms (Sierra et al., 2014).

neurodegenerative process depending on the context; however, it is generally accepted that M1 microglia aggravate the on-going neuropathology by producing neurotoxic factors, while M2 microglia help to resolve the problem via phagocytosis of unwanted molecules (Fig. 5) (Kim et al., 2013; Cherry et al., 2014). For example, classical activated microglia- derived proinflammatory cytokines such as IL-1β and TNF-α reduce the number of newborn cells in the neurogenic centers and impede normal synaptic activity in neurons (Ekdahl et al., 2003; Pickering et al., 2005; Walter et al., 2011) as observed frequently in ageing and neurodegenerative disorders. High dose of nitric oxide and reactive oxygen species also contribute to microglia induced neural apoptosis (Colton and Gilbert, 1987; Liu et al., 2002). These M1 microglia derived proinflammatory signals also stimulate neighboring astrocytes to proliferate and produce cytotoxic factors, resulting in more severe neuroinflammation (von Bernhardi and Eugenin, 2004). By contrast, several studies have proved that phagocytotic ability of alternative activated microglia is important to prevent/delay the development of neurodegeneration by removing the causative agents in several neurologic disorders (such as amyloid beta in Alzheimer`s disease) and restricting the affected lesions (Kiyota et al., 2010; Komohara et al., 2008). Therefore, comprehensive understanding of microglial roles in various neuropathologic conditions has to be preceded before testing the therapeutic potential of modifying microglial activity.

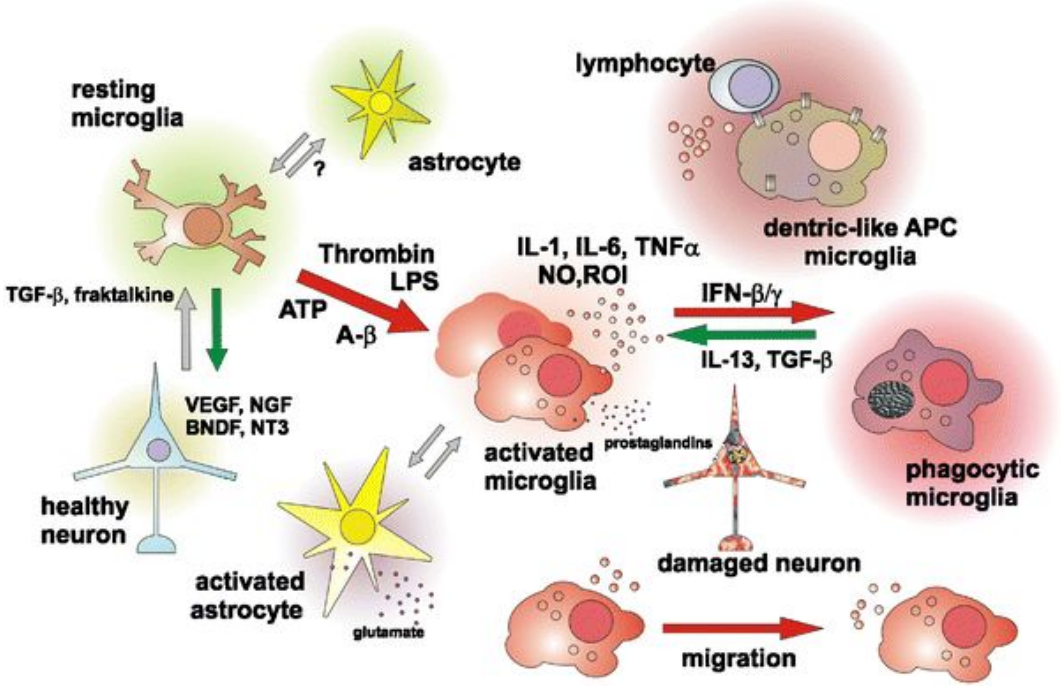

Figure 5. A schematic diagram of microglial activity in the neurodegenerative process.

Activated microglia can adopt a number of phenotypes including cytokine-secreting, phagocytic, and antigen-presenting cells. All of these different microglia phenotypes interact with each other as well as with astrocytes via the diffusible inflammatory mediators to produce a coordinated neuroinflammatory response (Kim et al., 2013).

In the field of NPC therapeutics, contribution of microglial activation in NPC development has been underestimated because NPC-affected neurons seem to undergo cell autonomous death (Ko et al., 2005). It is supported by previous findings showing that newborn-derived NPC1-deficient microglia cannot cause neuronal death in a co-culture in vitro system (Peake et al., 2011) and specific rescue of NPC1 gene in glial population is insufficient to prevent Purkinje cell loss in the NPC1 affected cerebellum (Lopez et al., 2011). Therefore, neurodegenerative process in NPC may begin in a glial-independent manner. However, considering the previous report showing that chronic administration of non-steroidal anti-inflammatory drug ibuprofen provided a meaningful amelioration of motor dysfunction in NPC1 mice (Smith et al., 2009), regulation of microglial activation can be considered as one of NPC therapeutic approaches to reduce/manage the clinical manifestations.

PART I

hUCB-MSCs AMELIORATE NEUROPATHIES IN NPC1

1.1 INTRODUCTION

Niemann-Pick disease type C (NPC) is a fatal genetic disorder with an incidence estimated at between 1:120,000 and 1:150,000 live births (Meikle et al., 1999; Vanier and Millat, 2003). NPC is caused by the mutation of NPC1 gene (95 % of cases; referred to as NPC1) or NPC2 gene (rest of cases; referred to as NPC2) (Carstea et al., 1997), which encodes a transmembrane protein of the late endosome and lysosome (LE/L). As NPC1/2 proteins facilitate the movement of unesterified cholesterol derived from the cellular uptake of lipoproteins (Liu et al., 2007), mutations in those proteins result in excessive accumulation of cholesterol within the LE/L (Loftus et al., 1997). In the aspect of neurodegenerative disease, the phenotypes of both NPC1 and NPC2 are characterized by distended neurons, demyelinated axons, reactive gliosis and neuronal loss, eventually leading to dystonia, ataxia, seizures, dementia and premature death (Baudry et al., 2003a; Paul et al., 2004b; Sturley et al., 2004). Although some chemicals such as cyclodextrin (Griffin et al., 2004) or Miglustat (Lachmann et al., 2004; Patterson et al., 2007) have been suggested as a potential therapeutic agent to manage neurological symptoms of this fatal disease, more researches are needed in the field of NPC therapeutics.

Currently, stem cell transplantation has emerged as a promising therapeutic approach for neurodegenerative disorders and a number of studies have shown that not only neural stem cells but also embryonic or mesenchymal stem cells (MSCs) contribute to correct the neurological abnormalities (Cho et al., 2009; Glavaski-Joksimovic et al.,

2009; Lindvall and Kokaia; Lindvall et al., 2004; Torrente and Polli, 2008). It has been reported that whole hUCB (human umbilical cord blood) contains highly immature cells with extensive proliferation capacity (Leung et al., 1999) and hUCB-MSCs also maintain stemness and multipotency based on Oct4A function (Seo et al., 2009). In addition, administration of whole hUCB cells or hUCB-MSCs provides beneficial effects to animal models with neurodegenerative disorders including Alzheimer`s disease (AD) (Nikolic et al., 2008), Parkinson's disease (PD), amyotrophic lateral sclerosis (ALS) (Blandini et al.; Chen and Ende, 2000; Ende and Chen, 2002; Ende et al., 2000) and ischemia (Koh et al., 2008), implying that it would be of interest to study whether hUCB-MSCs can also improve NPC symptoms.

Therefore, I aimed to determine the therapeutic potential of hUCB-MSCs in NPC1 condition using transgenic mouse model. In this purpose, I transplanted hUCB-MSCs into the hippocampus of transgenic NPC1 mice model at the age of 4 weeks. It is noted that hUCB-MSC treated NPC1 mice showed recovery of motor dysfunction. In histological analysis, intracellular cholesterol accumulation was significantly reduced with increased neurogenesis in the dentate gyrus (DG) after transplantation of hUCB-MSCs. I also revealed that hUCB-MSCs activated PI3K/AKT and JAK2/STAT3 pathway signaling and altered neurotransmitter transporter expression toward reducing the excitotoxicity. The overall data support the availability of hUCB-MSCs based therapy in NPC1 and in other neurodegenerative diseases.

1.2 MATERIALS AND METHODS

(1) Isolation and maintenance of hUCB-MSCs

Isolation, culture and characterization of hUCB-MSCs were performed as described previously (Park et al., 2009; Seo et al., 2009). hUCB samples were obtained from the Seoul City Borame Hospital Cord Blood Bank. Samples from term and pre-term deliveries were harvested at the time of birth with the mother's informed consent. This work was approved by the Borame Hospital Institutional Review Board and Seoul National University (IRB No. 0603/001-002-07C1). The blood samples were processed within 24 hours of collection. The mononuclear cells were separated from the UCB using Ficoll-Paque TM PLUS (Amersham Bioscience, Uppsala, Sweden) and were suspended in a culture medium DMEM (Gibco, Grand Island, NY, USA), containing 20% fetal bovine serum (FBS), 100 I/ml penicillin, 100 mg/ml streptomycin, 2 mM L-glutamine, and 1 mM sodium pyruvate.

(2) In vitro differentiation and flow cytometric analysis of hUCB-MSCs

For osteogenic differentiation, hUCB-MSCs were maintained in DMEM, containing 100 nM dexamethasone, 50 μM ascorbic acid, 10 mM β-glycerophosphate supplemented with 10 % FBS, then they were immunostained with Alizarin red S. For adipogenic differentiation, hUCB-MSCs were cultured in DMEM supplemented with 5 % FBS, 1 μm dexamethasone, 10 μm insulin, 200 μm indomethacin, 0.5 mm isobutylmethylxanthine for 3 weeks followed by Oil Red O staining. For chondrogenic

differentiation, hUCB-MSCs were cultured with DMEM containing 3.5 g/ml glucose, 1% (v/v) ITS (Sigma-Aldrich), 2 mM L-glutamine (Invitrogen), 100 μg/ml sodium pyruvate, 0.2 mM ascorbic acid 2-phosphate (Sigma-Aldrich), 10^{-7} M dexamethasone (Sigma-Aldrich), and 10 ng/ml transforming growth factor-β3 (R&D Systems) medium. After 3-4 weeks, the differentiated cells were immunostained with Toluidine blue. For Flow Cytometric analysis, the cells were detached and fixed with 70 % ethanol for 10 min at 4°C. They were stained with each FITC- or phycoerythrin conjugated antibodies (BD Bioscience) at 4°C for 30 min. Thereafter, the cells were washed twice and resuspended in 1 ml of PBS and were immediately analyzed using Flow Cytometry (FACSAria, Becton Dickinson).

(3) Cytokine array analysis

At 80 % confluence, the culture medium of the hUCB-MSCs was switched to serum-free culture medium DMEM for 48 hours and the conditioned medium was collected for analysis of the cytokine expression. Cytokines, secreted by the hUCB-MSCs, were determined using RayBio® Human cytokine Antibody Array 3 and 5 (RayBiotech, Norcross, GA, USA) according to the manufacturer's instructions. The positive controls on membrane were used to normalize the signal intensity of individual cytokines.

(4) Animal models

NPC1 transgenic mice were obtained from breeding pairs of Balb/c NPC1^{NIH} mice purchased from Jackson Laboratories (Bar Harbor, MA, USA). The genotyping was

performed as previously described (Yang et al., 2006). All experiments were approved and followed by the regulations of the Institute of Laboratory Animals Resources (SNU-090819-3, Seoul National University, Korea).

(5) Transplantation of the hUCB-MSCs into NPC1 mice

The mice (four weeks old) were randomly divided into four groups: hUCB-MSCs transplanted NPC1 mice (n = 16), vehicle injected control NPC1 mice (VC-NPC1; n = 10), un-treated control NPC1 mice (n = 11) and wild-type control mice (WT; n = 12). Anesthesia was induced with 5 % isoflurane and maintained with 2 % isoflurane administered through a facial mask. The hUCB-MSCs were transplanted into the hippocampus using the stereotaxic apparatus and Ultra-micropump (World Precision Instruments, Sarasota, FL, USA). To track injected hUCB-MSCs, three of NPC1 mice were given cells labeled with membrane-bound fluorescent marker PKH26. The injection coordinates were 2.00 mm posterior, 1.40 mm bilateral to bregma and injection depth was 2.00 mm. Each recipient received approximately 1 $x10^6$ cells in 2 μl of cell suspension with phosphate buffered saline (PBS) at a rate of 500 nl per minute. For sham control, animals underwent the same transplantation procedure but received vehicle infusion of equal volume of PBS. After the transplantation, scalp was closed by suture and animals were recovered from the anesthesia.

(6) Rotarod test

Motor coordination test was assayed using a Rota Rod treadmill (7650

Accelerating model, Ugo Basile Biological Research Apparatus, Comerio, Italy). Mice were first trained at the age of 3 weeks during one week. After the training, mice were subjected to the Rota Rod test at 10 rpm every week from 5 to 7 weeks of age. The test was performed once per week and the mean record was adopted as the performance time of three attempts.

(7) RNA extraction and RT-PCR

Total RNA was extracted from mice brain using Easy-spin total RNA extraction kit (Intron Biotechnology, Seoul, Korea) according to the manufacture's protocol. The cDNA was then amplified in a PCR reaction containing 5-10 pM of specific primers. Primer sequences were designed using Primer Express software (PE-Applied Biosystems, Warrington, UK) with gene sequences obtained from the GeneBank database. The primer sets used were as follows: ATP-binding membrane cassette transporter A1 (ABCA1) (F: 5`- CGTTTCCGGGAAGTGTCCTA-3'; R: 5'- GCTAGAGATGACAAGGAGGATGGA-3`), ATP-binding membrane cassette transporter G5 (ABCG5) (F: 5'- GTCCTGCTGAG-GCGAG-TAAC-3'; R: 5'- GCAGCATCTGCCACTTATGA-3'), Liver X receptor α (LXRα) (F: 5'- AGGAGTGTCGACTT-CGCAAA-3'; R:5-CTCTTCTTGCCGCTTCAG-TTT-3') and GAPDH (F: 5′-TGAAGCAG-GCATCTGAGGG-3′ ; R:5′-CGAAGGTGGA-AGAGTGGGAG-3′).

(8) Protein extraction and western blot analysis

The brains of mice 7-8 weeks old were taken and divided into

cerebrum/cerebellum or cortex, striatum, hippocampus and cerebellum following experimental purposes. Each tissue homogenized independently in lysis buffer containing protease inhibitor cocktail (Roche Applied Science, Mannheim, Germany), followed by vigorous shaking for a few minutes in the presence of 20 µl of 10 % Nonidet - P40. The total protein content of each lysate was quantified using a Bio-Rad protein assay kit (Bio-Rad Laboratories, Foster City, CA, USA). For western blotting, equal amount (30 µg) of protein extracts were subjected to 8-15 % SDS-PAGE analysis and transferred to a nitrocellulose membrane for incubation with primary antibodies. After immunoblotting with secondary antibodies, proteins were detected with enhanced chemiluminescence reagent (Intron Biotechnology). The relative band intensities were determined using NIH ImageJ version 1.34e software. One representative band from three independent experiments was chosen for presentation. The following primary antibodies were used: anti-Phosphoinositide3-kinase (PI3K), anti-phosphoPI3K (pPI3K), anti-AKT, anti-phosphoAKT (pAKT), anti-phospho Janus kinase2 (pJAK2), anti-phospho Signal Transducers and Activators of Transcription protein3 (pSTAT3) Tyr705, anti-pSTAT3 ser727, anti-Glycogen synthase kinase3β (GSK3β), anti-pGSK3β Ser9 (Cell signaling, Danvers, MA, USA); anti-pSTAT3 Ser 727, anti-Excitatory Amino Acid Transporter2 (EAAT2), anti-microtubule associated protein2 (MAP2), anti-glial fibrillary acidic protein (GFAP), anti-doublecortin (DCX), anti-calbindin (CBD), anti-3-hydroxy-3-methylglutaryl coenzyme A reductase (HMGR) (Millipore, Billerica, MA, USA); anti-glutamic acid decarboxylase65 (GAD65), anti-GABA transporter1 (GAT1) (Abcam, Cambridge, MA, USA); anti-JAK2, anti-Excitatory Amino Acid Transporter3 (EAAT3)

(Santa Cruz Biotechnology Inc., Delaware, CA, USA) ; and anti-β-actin (Sigma-Aldrich).

(9) Immunohistochemistry

Mice were perfused with 0.1 M PBS (pH 7.4), followed by 4% paraformaldhyde in 0.1 M PBS, and brains were isolated carefully and soaked in 4% paraformaldhyde in 0.1 M PBS overnight for post-fixation. They were prepared for paraffin section to obtain 4 μm-thick sections for H&E staining. For immunohistochemistry, the brain tissues were transferred to a mold filled with infiltration mixture (OCT compound) (Sakura Finetek, Tokyo, Japan) and kept at -70°C overnight until cryosection on a cryostat (CM 3050, Leica, Wetzlar, Germany). Primary antibodies incubated with the sections were: anti-DCX, anti-MAP2, anti-GFAP, anti-human mitochondira (HuMi), anti-CBD (Milipore). Subsequently, the sections were extensively washed with PBS and 1 hour incubation with anti-mouse or rabbit secondary antibodies conjugated with Alexa Fluor 488 / 594 (Molecular Probes; Eugene, OR, USA), followed by Hoechst 33238 (1 μg/ml, Sigma-Aldrich) staining in order to visualize the cell nuclei. Images were captured and merged on a confocal microscope system (Eclipse TE200, Nikon, Nagano City, Japan). To compare the degree of cholesterol accumulation, we performed filipin staining as the previous methods (Kim et al., 2007; Kobayashi et al., 1999), then depicted hippocampal, cortical and striatal region from each group (n=5). NIS element software (Nikon) was used to analyze intensity of staining.

(10) Whole-cell patch clamp recordings

4 weeks post transplantation, the brains were placed in ice-cold, oxygenated (95% O_2/5% CO_2) low-Ca^{2+}/high-Mg^{2+} slicing solution composed of (in mM): 5.0 KCl, 7.0 $MgCl_2$, 28.0 $NaHCO_3$, 1.25 NaH_2PO_4, 0.5 $CaCl_2$, 7.0 glucose, 3.0 pyruvic acid, 1.0 ascorbic acid, and 234.0 sucrose. After sectioning, the slices (300 μm in thickness) were pre-incubated in the artificial cerebrospinal fluid. For recordings, a slice was transferred to a submersion-type recording chamber continuously perfused with the 95 % O_2/5% CO_2-saturated standard artificial cerebrospinal fluid at 34–35°C. Individual hippocampal cells were viewed with an Olympus microscope fitted with a 40X water-immersion objective and differential interference contrast optics (Olympus, Tokyo, Japan). Whole-cell patch-clamp recordings were made using an Axopatch 200B patch-clamp amplifier (Axon Instruments, Foster City, CA, USA). The recording pipettes were pulled from borosilicate capillaries (1.5 mm OD, 1.0 mm ID; WPI) using a micropipette puller (Narishige, Tokyo, Japan). The resistance of the pipette was 4 to 6 MΩ when it was filled with a solution containing (in mM): 130.0 potassium gluconate, 1.0 $MgCl_2$, 10.0 HEPES, 10.0 EGTA, 1.0 $CaCl_2$, and 4.0 adenosine triphosphate-Mg adjusted to pH 7.25 with 1 M KOH (290–320 mOsm). The solutions were perfused at a rate of 3–4 ml/min at 34–35°C. A tight GΩ seal was obtained on the neuron identified. Recordings began ~5 min after whole-cell access was obtained and the current reached a steady state. The series resistance ranged from 15 to 30 mΩ as estimated directly from the amplifier. The data were digitized by Digidata 1200B (Axon Instruments). The recording was abandoned if the input resistance changed more than 15 % during the recording.

(11) Statistical analysis

Results are shown as means ± SE. Statistical analysis of significance was calculated by one-way ANOVA followed by Bonferroni post-hoc test for multigroup comparisons (StatView 5.0; SAS Institute, Cary, NC). Statistical significance is indicated in the figure legends.

1.3 RESULTS

(1) Characterization of hUCB-MSCs

To determine the multi-lineage differentiation potential of hUCB-MSCs, hUCB-MSCs were controlled under lineage specific culture conditions. The hUCB-MSCs were able to differentiate into multi-lineages which are osteogenic-, adipogenic-, and chondrogenic lineages (Figs. 6A, C, E, control; Figs. 6B, D, F, induction of multi-lineage differentiation). I next determined proliferation ability and immunological phenotypes of hUCB-MSCs. In cumulative population doubling assay, hUCB-MSCs were able to achieve more than 35 cumulative population doublings (Fig. 6G). In a Karyotype test, no chromosomal abnormalities were found (Fig. 5H) and in cell surface antigen profiles, hUCB-MSCs were positive for CD24, CD29, CD44, CD73, CD90, CD105, and negative for CD10, CD14, CD31, CD34, CD45, CD62P, CD133, and HLA-DR (Table 1). To determine whether particular cytokines are released from hUCB-MSCs, I performed a quantitative cytokine analysis. The results of cytokine array revealed that hUCB-MSC conditioned medium contained considerable amounts of immune modulatory- and neurotrophic growth factors, such as IL-10, TIMP1 and 2, FGF, GDNF, BDNF and NGF (Fig. 7). These data suggest that hUCB-MSCs could be readily expanded and have multi-lineage differentiation potential with cytokine release.

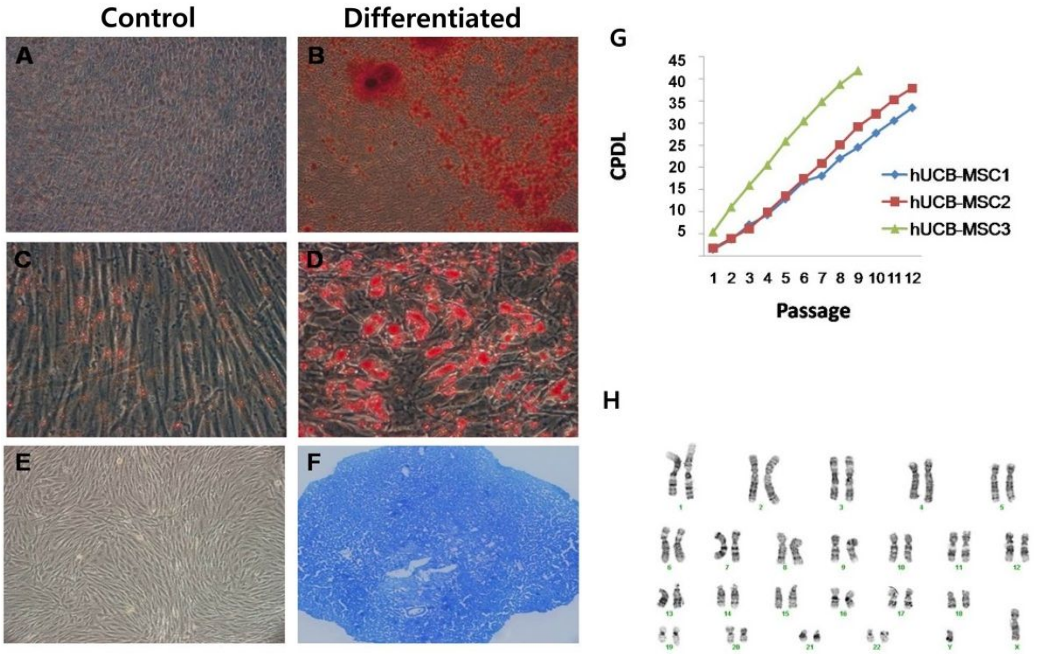

Figure 6. The characterization of hUCB-MSCs.

hUCB-MSCs differentiated into osteogenic (B), adipogenic (D), and chondrogenic (F) lineages. The undifferentiated controls are shown in (A), (C), and (E), respectively. Scale bars: 200 μm. (G) The cumulative population doubling level (CPDL) were achieved more than 35 cumulative population doublings. (H) In a karyotype test, no chromosomal abnormalities were found.

Table 1. The Phenotype Determination of hUCB-MSCs using Flow cytometry

Surface marker	hUCB-MSCs (%)
CD10	0.2 ± 0.1
CD14	2.0 ± 1.0
CD24	68.7 ± 2.9
CD29	100 ± 0.0
CD31	0.4 ± 0.7
CD33	4.8 ± 5.9
CD34	3.5 ± 3.4
CD44	100 ± 0.1
CD45	0.0 ± 0.1
CD51/61	6.4 ± 10.8
CD62P	0 ± 0
CD73	99.6 ± 0.5
CD90	99.7 ± 0.3
CD105	99.5 ± 0.8
CD133	0.1 ± 0.1
HLA-DR	2.0 ± 3.2

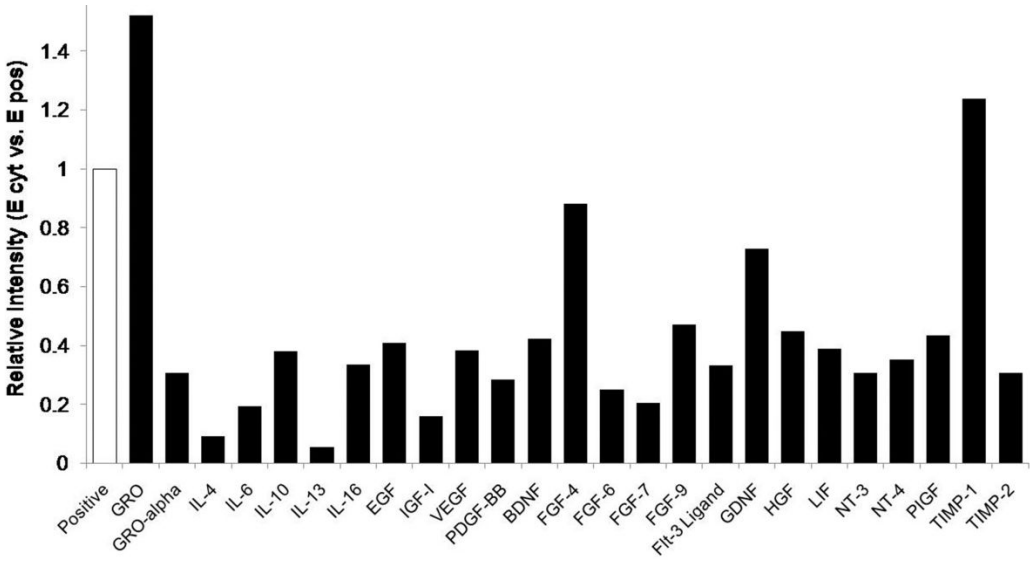

Figure 7. hUCB-MSCs released various immunomodulatory substance, neurotrophic cytokines, and growth factors.

Released soluble factors of hUCB-MSCs were analyzed by cytokine array. The positive controls on membrane were used to normalize the signal intensity of individual cytokines.

(2) hUCB-MSCs ameliorated altered cholesterol metabolism in cerebrum of NPC1 mice.

To determine whether the lysosomal cholesterol accumulation is ameliorated by engrafted hUCB-MSCs, filipin staining was performed in NPC1 mice. The quantitative analysis of the filipin positive area in hippocampus, motor cortex and striatum at postnatal day 56 revealed that hUCB-MSCs treated NPC1 mice showed significantly decreased cholesterol deposition (Figs. 8A-B). Each area occupied by filipin was 2.99 ± 0.5, 2.05 ± 0.35, 4.49 ± 0.85 % in NPC1 mice, while hUCB-MSCs treated NPC1 mice had, respectively, 2.33 ± 0.59 %, 1.12 ± 0.38 %, 2.56 ± 0.93% filipin-positive area (n=3 per group). To explain what led to this reduction, I evaluated mRNA expression level of sterol transport system related genes, such as LXRα, ABCA1 and ABCG5. As shown in Figure 8C, mRNA levels of ABCA1, ABCG5 and LXRα were hardly detectable in VC-NPC1 brain, whereas they were up-regulated mild to significant after hUCB-MSCs treatment. Moreover, hUCB-MSCs could lower the cholesterol synthesis by reducing protein expression of the rate limiting enzyme of cholesterol synthesis, HMGR (Fig. 8D).

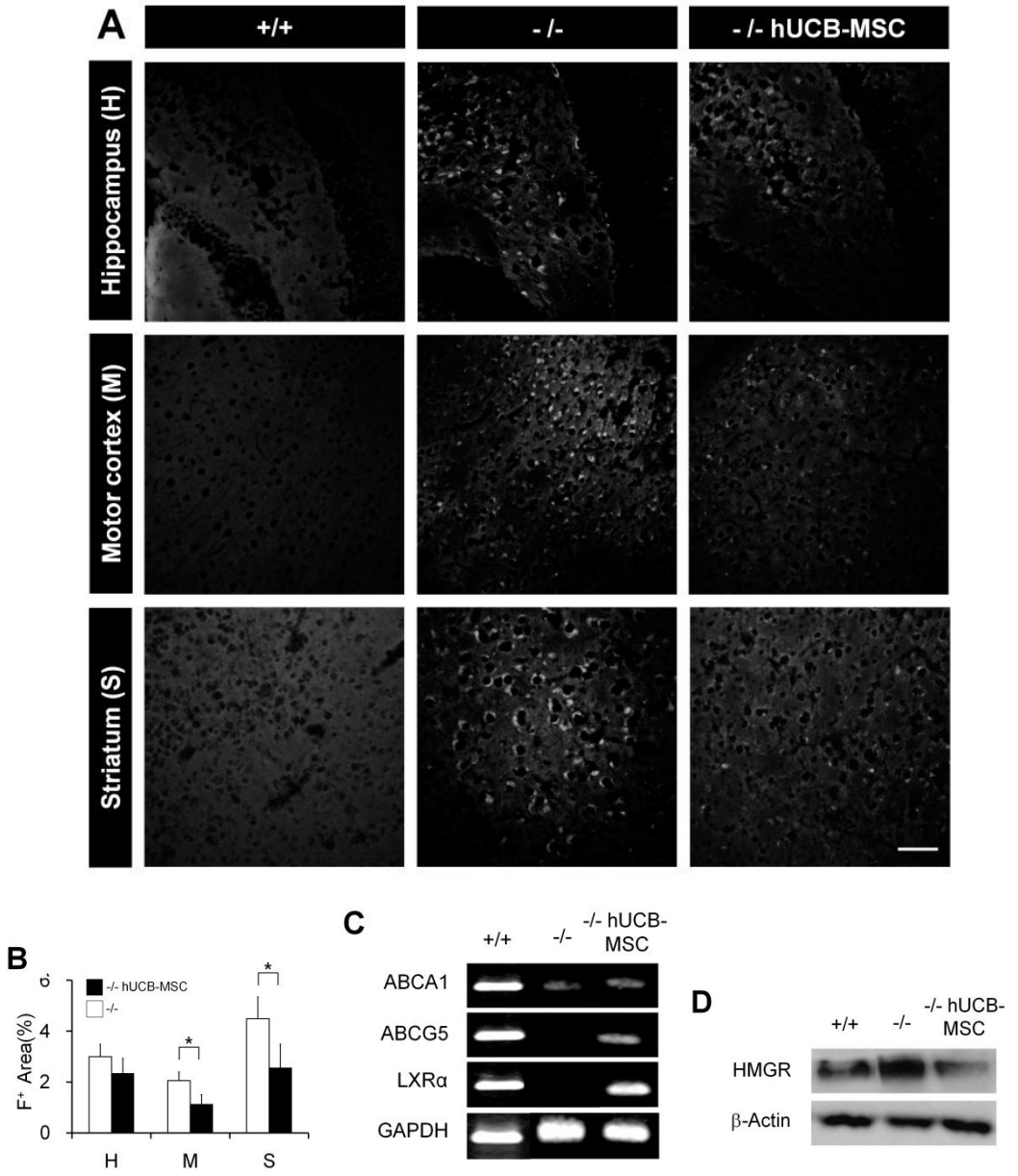

Figure 8. hUCB-MSCs restored the altered cholesterol metabolism and trafficking in NPC1 mice.

(A) The cholesterol accumulation was determined by anti-filipin staining images. Scale

bar: 50 μm. (B) Quantitative analysis of the filipin-positive areas between untreated and hUCB-MSC-treated NPC mice (mean ± SD, *p > 0.05) (n = 3 for each category). (C) mRNA level of ABCA1, ABCG5, LXRα, and GAPDH using RT-PCR. (D) Protein level of HMGR using western blot analysis. +/+, wild type mice; −/−, NPC mice; −/−hUCB-MSCs, hUCB-MSC-transplanted NPC mice.

(3) The engrafted hUCB-MSCs improved motor deficits in NPC1 mice

To evaluate motor function of the mice, the Rota-Rod test was performed. The performance was assessed once per week for 3 weeks after the transplantation. In every challenge, WT mice completed the task for 180 seconds (data not shown). As shown in Figure 9, hUCB-MSCs transplanted NPC1 mice could endure on the machine for 155.25 ± 25.89, 128.41 ± 22.26 and 89.83 ± 11.88 seconds at 7, 14 and 21 days post transplantation respectively, whereas relatively lower records were obtained from both vehicle treated-NPC1 mice (91.86 ± 16.17, 74.38 ± 9.32, 41 ± 7.23 s) and untreated NPC1 mice (130.63 ± 24.5, 98.88 ± 17.46, 56.75 ± 15.38 s). These data suggest that hUCB-MSCs improved an impaired motor function in NPC1 mice.

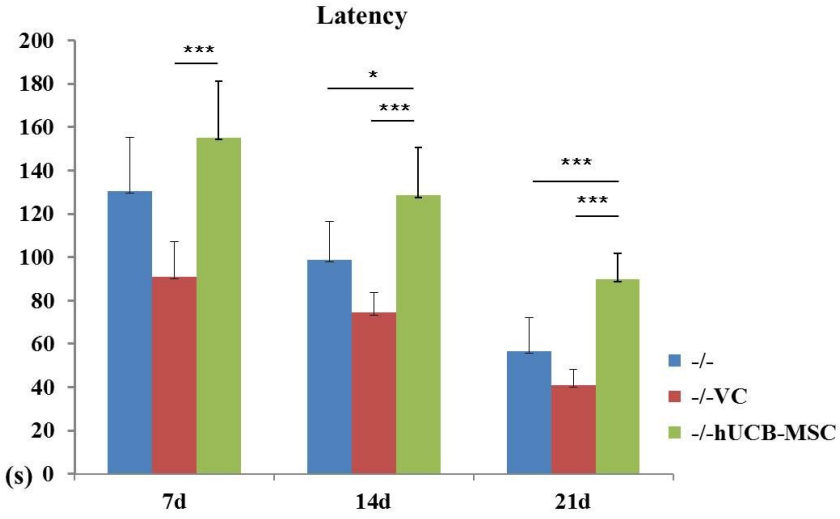

Figure 9. hUCB-MSCs improved motor function in NPC1 mice.

Locomotion ability of hUCB-MSC transplanted NPC1 mice showed significant improvement (*$p < 0.05$; ***$p < 0.001$). The test was performed once per week for 3 weeks post transplantation. d, days after transplantation.

(4) Cerebellar Purkinje cell survival was increased by hUCB-MSCs transplantation

The cerebellum is one of the most severely affected areas in the brain of NPC1 affected patients and animal models and Purkinje cells are exceedingly susceptible to the neurodegeneration (Ong et al., 2001; Sarna et al., 2003a). Therefore, I determined whether transplanted hUCB-MSCs prevented Purkinje cell loss in the cerebellum of NPC1 mice. The H&E staining in Figure 10A showed that significant reduction in the number of Purkinje cells was observed in both untreated- and VC-NPC1 mice, while hUCB-MSCs seemed to prevent Purkinje cell loss. This phenomenon was confirmed by immunohistochemistry and western blotting using a Purkinje cell marker CBD (Figs. 10 B-D). I next investigated whether protection effect on the Purkinje cells is associated with the suppression of apoptotic- and inflammatory signaling. As depicted in Figure 10E, protein levels of pro-apoptotic Bax and cleaved caspase-3 were moderately attenuated and inflammatory molecules including iNOS, F4-80 and COX2 were also decreased after hUCB-MSCs transplantation. These data suggest that hUCB-MSCs protect Purkinje neuronal population through providing anti-apoptotic- and anti-inflammatory effects in the NPC1-affected cerebellum.

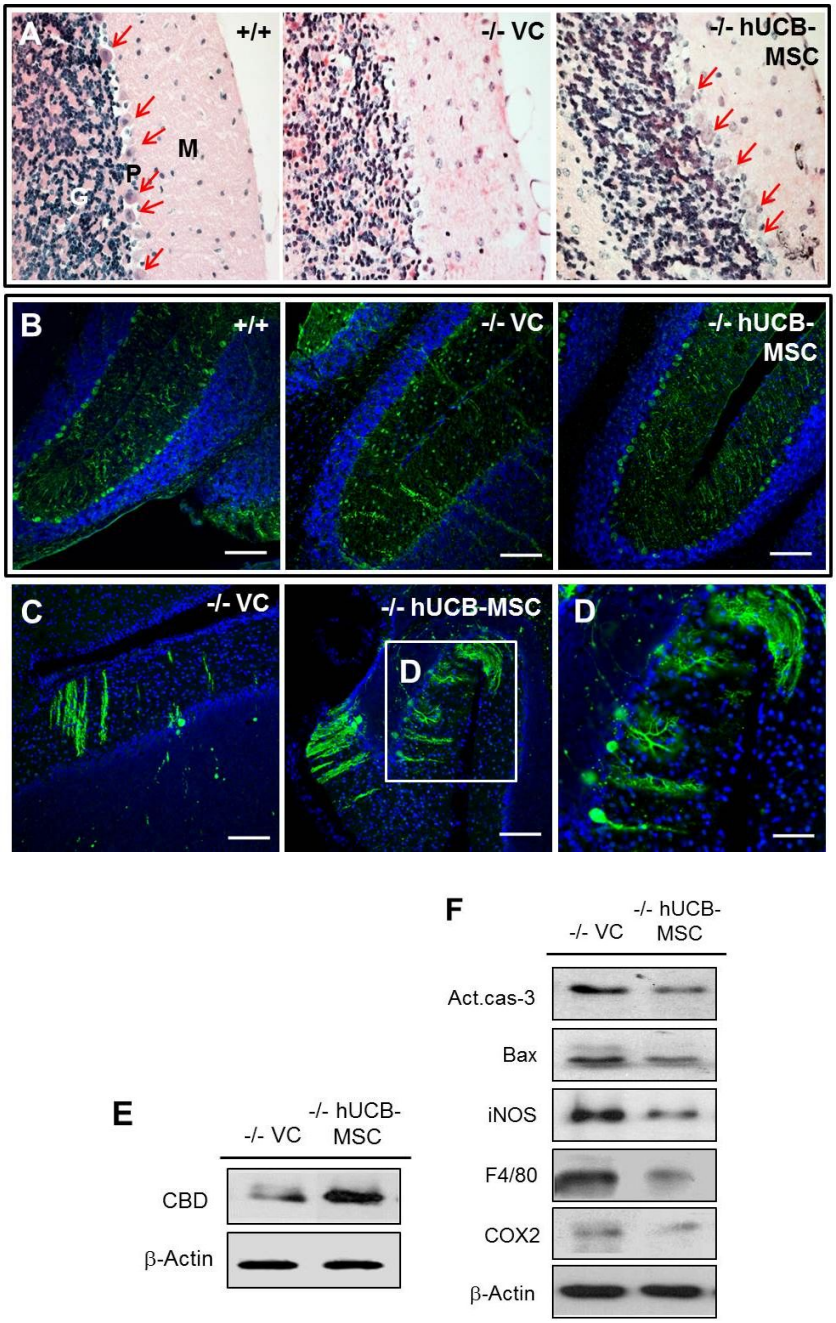

Figure 10. hUCB-MSCs prevented Purkinje cell loss and cerebellar inflammation.

(A) Purkinje neurons are indicated by arrows in H&E staining. (B, C) Purkinje cells were

labeled with anti-CBD in immunohistochemistry. Nuclei were counterstained with Hoechst 33258. Scale bars: 50 μm. (D) Protein level of CBD was determined by western blot analysis. (E) Western blot analysis of activated caspase-3, BAX, iNOS, F4/80, and COX2 were decreased when the hUCB-MSCs were transplanted in NPC1 mice.

(5) hUCB-MSCs drove neurogenesis and differentiated into functional neurons

Since DG is a site of neurogenesis in the brain (Kuhn et al., 1996), I examined the influence of hUCB-MSCs on *de novo* neurogenesis using immunohistochemical analysis. At post 3 weeks of the transplantation, it is revealed that more DCX-positive neural progenitors were present in the DG of the hUCB-MSC treated NPC1 mice compared to other group (Fig. 11A). Further, protein levels of DCX and mature neuronal marker MAP2 were readily increased only in hUCB-MSCs transplanted samples whereas no significant change in astrocyte protein GFAP was observed between groups (Fig. 11B).

To track the fate of transplanted cells *in vivo*, hUCB-MSCs within the mouse brain were labeled with human-specific marker HuMi using immunohistochemistry. As shown in Figure 12A, immunoreactivity of HuMi revealed the presence of transplanted cells in the cortex. Interestingly, they were often expressing the neural marker MAP2, whereas cells simultaneously expressing GFAP and HuMi were hardly detectable (Fig. 12B). Thus, I hypothesized that some of engrafted hUCB-MSCs underwent differentiation into neurons.

I next determined whether these hUCB-MSC-derived neurons have functional electrical and physiological activities using whole-cell patch-clamp recordings with hippocampal slices. For this experiment, hUCB-MSCs were pre-labeled with a cell membrane permeable dye PKH26 before transplantation for the convenience in finding treated cells *in vivo*. The recording site was hippocampal CA1 region and PKH26-labeled hUCB-MSCs were visually identified as shown in Figs. 12C-D. A train of action potentials was fired by injecting a depolarizing current (0.2 nA, 600 ms, upper panel in

Fig. 12E) into the PKH26 labeled cells and it was blocked by 1 μM of tetrodotoxin (TTX), a voltage-dependent Na channel blocker (lower panel in Fig. 12E). In addition, miniature excitatory postsynaptic currents, recorded in labeled neurons tested at a holding potential of -70 mV, were disappeared by 6-cyano-7-nitroquinoxaline-2, 3-dione (CNQX) and 2-amino-5-phosphopentanoic acid (AP5), used as a specific antagonist for AMPA and NMDA receptor, respectively (Fig. 12F). These data suggest that transplanted hUCB-MSCs were able to trans-differentiate into synapse associated, receptor-dependent neurons.

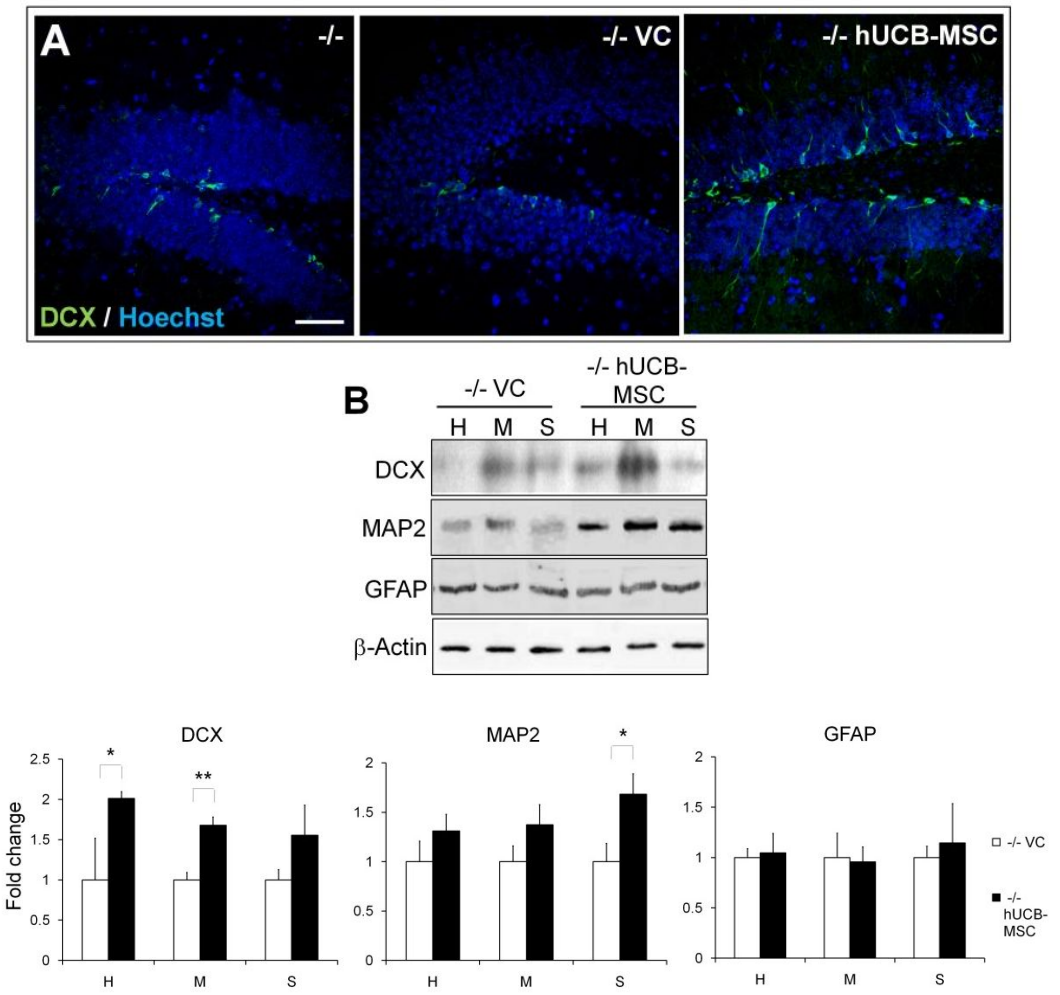

Figure 11. hUCB-MSCs increased neural progenitor cells.

(A) DCX^+ neural progenitor cells were determined by confocal microscope in dentate gyrus. Nuclei were counterstained with Hoechst 33258. Scale bar: 50 μm. (B) Proteins level of DCX at 3 weeks and of MAP2 and GFAP at 4 weeks post-transplantation were determined using western blot analysis. The immunoblots were quantified by densitometry and normalized β-actin levels in the same lane. *$p < 0.05$; **$p < 0.01$.

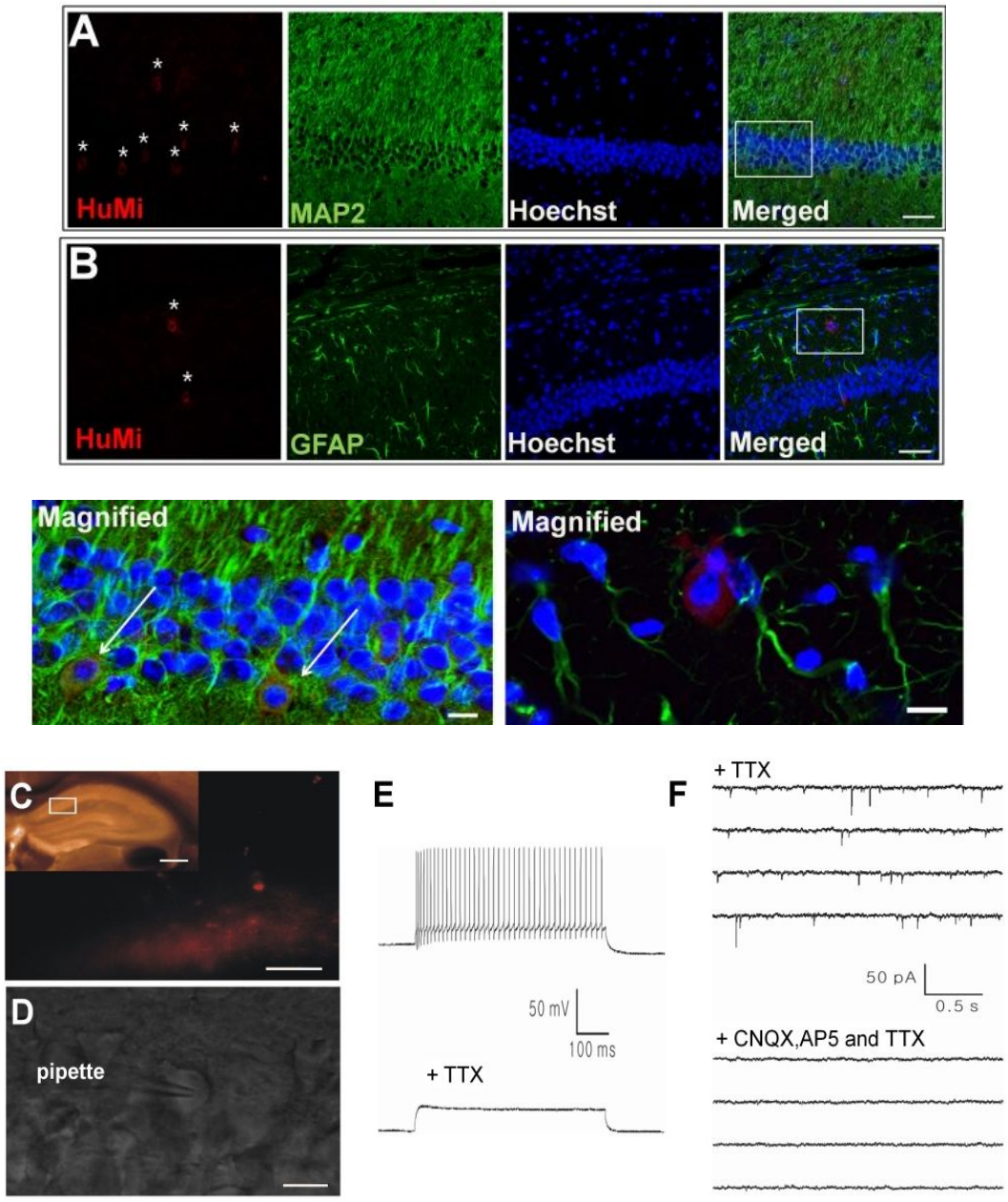

Figure 12. hUCB-MSCs differentiated into mature neurons with functional synapse in NPC1 mice.

(A, B) Asterisks indicate hUCB-MSCs labeled with HuMi. Neurons and astrocytes were

labeled with MAP2 and GFAP. Arrows indicate differentiated neurons derived from hUCB-MSCs. Magnified image of square is also shown. Scale bars: 50 μm (A, B), 10 μm (magnified images). (C) PKH26-labeled testing cells (red) are shown around the transplantation site. Scale bars: 250 μm (left, upper box), 20 μm (lower box). (D) A picture of the cell injection by pipette into the pyramidal CA1 region of the hippocampus. Scale bar: 10 μm. (E) Action potentials in donor-derived neurons induced by depolarization (upper panel) and inhibited by TTX (lower panel). (F) The miniature excitatory postsynaptic currents (upper panel) were abolished by CNQX and AP5 (lower panel).

(6) hUCB-MSCs promoted neuronal survival via up-regulation of PI3K/AKT and JAK2/STAT3 pathway and restored disrupted homeostasis of neurotransmitters in NPC1 mice

Since treatment of hUCB-MSCs seemed to attribute to neural protection in NPC1 mice, I examined several signaling pathways known to be involved in neuronal protection such as PI3K/AKT and JAK2/STAT3 cascade to identify hUCB-MSCs induced neuro-protective mechanism (Dziennis and Alkayed, 2008; Kaytor and Orr, 2002). In western blot analysis, PI3K/AKT signaling pathway was activated, followed by GSK3β inactivation via phosphorylation at Ser9 residue after hUCB-MSCs transplantation in both cerebrum and cerebellum of NPC1 mice at 4 weeks after transplantation (Fig. 13). JAK2/STAT3 phosphorylation was also increased in hUCB-MSCs transplanted NPC1 mice. These data suggest that PI3K/AKT and JAK2/STAT3 signaling pathway activated by hUCB-MSCs mediates neuroprotective effect in NPC1 mice.

We have shown that the expression of glutamate- and GABA transporter was altered in NPC1 mice compared with WT littermate (Byun et al., 2006). It has been known that inadequate or unbalanced neurotransmitter levels caused neurotoxicity. Therefore, I performed western blot analysis to determine whether hUCB-MSCs correct the impaired neurotransmitter homeostasis in NPC1 mice. In is noted that one of the GABA transporter GAT1 protein level was decreased while glutamate trafficking related GAD65, EAAT2 and EAAT3 protein levels were increased in hUCB-MSC transplanted NPC1 mice as compared with VC-NPC1 mice (Fig. 14). These data suggest that hUCB-MSCs might modulate transporter to reduce excitotoxicity in brain of NPC1 mice.

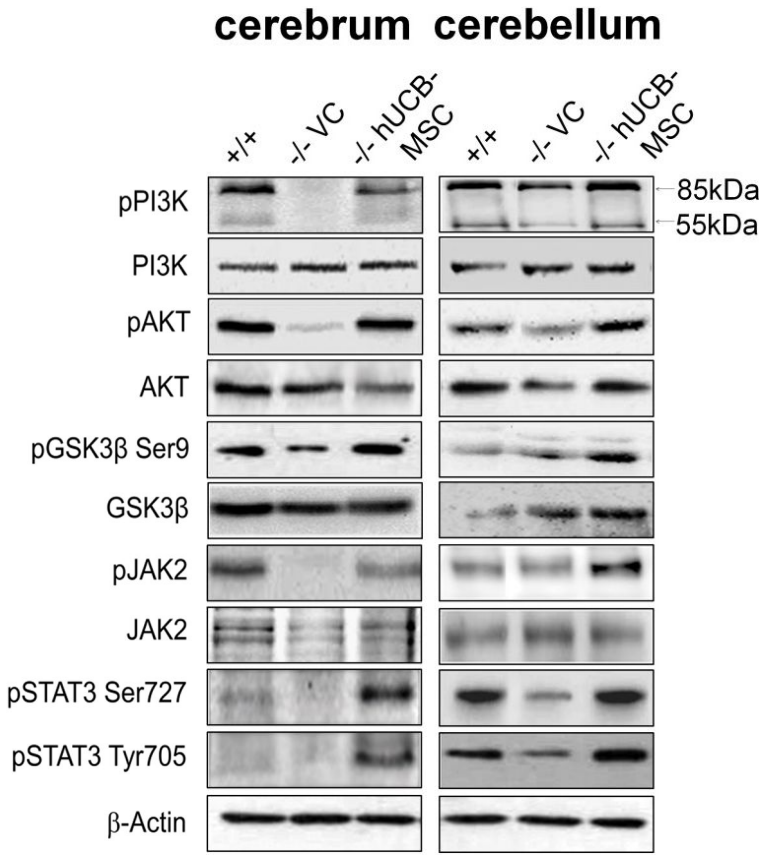

Figure 13. hUCB-MSCs promoted neuronal cell survival via up-regulation of PI3K/AKT and JAK2/STAT3 signaling pathways in NPC1 mice.

Protein levels of each signaling-related molecules and β-actin were determined in cerebrum and cerebellum of NPC1 mice by western blot analysis.

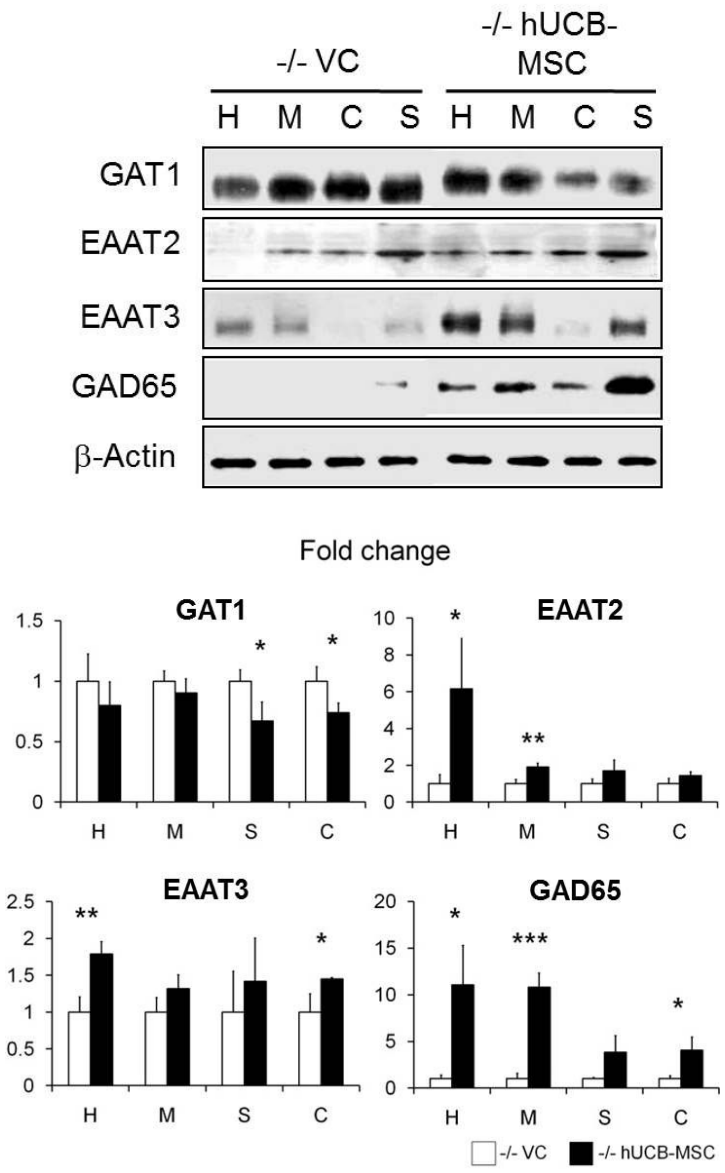

Figure 14. hUCB-MSCs modulated the GABA transporters in NPC1 mice.

Protein levels of GAT1, EAAT2, EAAT3 and GAD65 were determined by western blot analysis. Immunoblot was quantified by densitometry. *p < 0.05; **p < 0.01, ***p < 0.001.

1.4 DISCUSSION

In this study, I transplanted hUCB-MSCs into hippocampus of asymptomatic NPC1 mice and evaluated how the cells affected disease progression. I found that hUCB-MSCs brought several improvements in NPC1 mice, showing their potential as a therapeutic agent in neurodegenerative diseases.

Since hUCB-MSC was transplanted at the DG, one of neurogenic center in the brain, I firstly determined the alteration of endogenous neurogenesis after the transplantation. Nakano-Doi, A. *et al* have reported that systemically injected bone marrow mononuclear cells enhance proliferation of endogenous neural cells in cerebral infarction model (Nakano-Doi et al., 2010). Similarly, it is shown that systemic administration of hUCBs to stroke induced mice enhances neurogenesis (Taguchi et al., 2004). In keeping with earlier results, I revealed that hUCB-MSCs led to activate endogenous neurogenesis, indicated by increased DCX positive neural progenitors in the DG. The interesting point is that some of transplanted cells seemed to acquire neuronal phenotype. Even though the concept of 'transdifferentiation' has been a controversial issue and its significance or mechanism is not determined well, it is still worthy to report that hUCB-MSCs can differentiate into neuron with functional synapse in the NPC1-affected mouse brain.

In addition to beneficial effects of hUCB-MSCs around the injection site, hUCB-MSCs could rescue Purkinje neuron loss in the cerebellum. Purkinje cell is largest neuron

in brain and most vulnerable cell in NPC1 (Ko et al., 2005). Based on the fact that Purkinje neurons function as a coordinator of motor activity, mice with NPC1 perform poorly in the motor function related behavioral test such as rota-rod test (Higashi et al., 1993). My results indicated that hUCB-MSCs transplanted mice had more Purkinje cells in the cerebellum and as a result, they carried out a rota-rod task well compare to control NPC1 groups. Taken together, hUCB-MSCs could ameliorate the typical pattern of NPC1-related neurodegeneration in the cerebellum, followed by ultimate motor function recovery.

Cholesterol transport in the brain is essential for various functions including neuronal survival and the synthesis of neurosteroids (Orth and Bellosta, 2012). Aberrant cholesterol transport is linked to the early onset of NPC1 and the lipid accumulation is detected in neurons of the cerebral cortex, cerebellum, and hippocampus (Paul et al., 2004). In this study, I showed that hUCB-MSCs ameliorated altered cholesterol metabolism in the hippocampus, motor cortex and striatum of NPC1 mice through increasing cholesterol efflux transporters such as ABCA1, ABCG5 and their upstream LXR, as well as decreasing the production of cholesterol by HMGR. It has been reported that oral administration of LXR agonist slows progress of NPC1 symptoms through the activation ABCA1 and other cholesterol transporters (Repa et al., 2007). Thus, enhancement of cholesterol transport after hUCB-MSCs treatment would be an important aspect to explain hUCB-MSC derived benefit in NPC1 mice.

The fine balanced neurotransmitter homeostasis is one of the essential factors for adequate neuronal development, differentiation and communication (Levitt et al., 1997). I

especially focused on the level of glutamate and GABA, excitatory- and inhibitory neurotransmitters respectively, based on my previous data showing that protein expression level of GABA transporter GAT3 is increased in the hippocampus of NPC1 mice, while that of glutamate transporter EAAT2 is decreased (Byun et al., 2006). This tendency can lead to GABA/glutamate imbalance, known as glutamate induced toxicity. Glutamate toxicity has been posited to play a role in neurodegenerative disease including AD and reduced glutamate transporter and glutamate uptake were decreased in brains from patients with AD (Masliah et al., 1996). In this study, I described that NPC1 gene defect leads to reduce the mRNA level of Glutamate lowering molecules including EAAT2, GAD6 and EAAT3. Of interests, hUCB-MSCs could increase the mRNA levels of glutamate transporters, suggesting that hUCB-MSCs might contribute to homeostasis of the glutamate activity to combat excitotoxicity. Further study comparing the actual concentration of these neurotransmitters between WT, NPC1 control and hUCB-MSC treated NPC1 mice brain would be necessary to confirm this hypothesis.

Taken together, hUCB-MSCs ameliorated altered cholesterol metabolism by activation of cholesterol transporters, increased neuronal survival via activation of PI3K/AKT and JAK2/STAT3 signaling and prevented excitotoxicity in NPC1 mice. Moreover, hUCB-MSCs transplantation significantly increased neuronal progenitors, which differentiated into functional neurons in NPC1 mice. The transplanted hUCB-MSCs implied beneficial effects in preventing neuronal cell loss in the cerebrum and promoting Purkinje cells in the cerebellum, and eventually these effects improved motor function in NPC1 mice. Therefore, hUCB-MSCs could be a beneficial source for stem

cell therapy, and these studies could lead to a better understanding in a variety of neurodegenerative diseases.

PART II

ABNORMAL MICROGLIOSIS IMPAIRS OLFACTION IN NPC1

2.1 INTRODUCTION

The olfactory system is an essential sensory element for survival, and it is primarily based on well-organized neuronal communications between the olfactory epithelium (OE) and the olfactory bulb (OB). Every process associated with proliferation, maturation, integration and apoptosis of OB neurons must be fine-tuned to maintain olfaction functional integrity (Lledo et al., 2008; Nissant and Pallotto, 2011). Interestingly, the progressive loss of olfaction is often observed in the initial stages of neurological disorders, including Alzheimer's disease (AD) (Wilson et al., 2009), Parkinson's disease (PD) (Doty, 2012), dementia and Down's syndrome (McKeown et al., 1996; Murphy et al., 2002), which suggests that olfactory dysfunction is an early sign of neurodegeneration (Albers et al., 2006). The presence of amyloid-β (Aβ) or α-synuclein pathology has been linked to this phenomenon (Bahar-Fuchs et al., 2010; Beach et al., 2009). However, the pathological basis of olfactory dysfunction in the neurodegenerative process has not been thoroughly explained.

Niemann-Pick disease type C1 (NPC1) is a fatal metabolic disorder caused by a mutation in the NPC1 gene, which leads to the disruption of the lipid trafficking system and lipid sequestration within the lysosomal and late endosomal compartments (Carstea et al., 1997) . Considering that the presence of neurological complications is significantly correlated with disease severity (Vanier, 2010), elucidating the neurodegenerative process is an important step to establish therapeutic strategies for NPC1. A patterned neuropathy

has been observed in NPC1-affected humans and mouse models with distinctive signs of inflammation usually triggered by activation of microglia and/or astroglia (Ong et al., 2001; Vanier, 2010). Because a neural-specific loss of the NPC1 gene is sufficient to reproduce the NPC1 phenotype (Elrick et al., 2010), neuronal damage might precede reactive microgliosis and astrocytosis in NPC1. However, several studies have also shown that a neural pathology could develop in a non-autonomous manner in NPC1 (Erickson, 2013). Indeed, intact NPC1 function in astrocytes seems to be important in supporting neurons *in vitro* (Chen et al., 2007), and NPC1 gene-null oligodendrocytes fail to maintain proper CNS myelination patterns, which results in Purkinje cell loss in the cerebellum that resembles NPC1 pathology (Yu and Lieberman, 2013). Furthermore, TNF-α, a pro-inflammatory cytokine, is involved in NPC1-associated liver damage (Rimkunas et al., 2009), and anti-inflammatory agents relieve symptoms and increase the life span of NPC1 mutant mice (Smith et al., 2009). Therefore, the role of abnormal microgliosis and inflammation in NPC1 progression still needs to be determined.

Herein, I assessed the pathological changes in olfaction using an NPC1 mouse model. My results demonstrated that NPC1 mice showed distinct signs of olfactory dysfunction in a behavior test compared with WT controls. My results also revealed a drastic loss in olfactory sensory neurons (OSNs) and neuroblasts with excessive microglial activation in the NPC1-OB. Notably, the administration of the anti-inflammatory drug CsA considerably improved olfactory function and increased neural survival in NPC1 mice through microglial inhibition. These data indicate that the regulation of microglial activation might be important for the treatment of olfactory

dysfunction in neurological disorders.

2.2 MATERIALS AND METHODS

(1) Animal model

Breeding pairs of heterozygous NPC1 null mice (Balb/c $NPC1^{NIH}$; NPC1) were purchased from Jackson Laboratories (Bar Harbor, MA). The genotyping was performed as previously described (Seo et al., 2011), and homozygous WT and NPC1 mice were used in this study. All animals were handled in accordance with the regulations of the Institute of Laboratory Animals Resources (SNU-110517-3, Seoul National University, Korea). No specific gender-based differences were observed in each experiment. The number of animals used is indicated in the Results and Figure Legend sections.

(2) Buried food finding test

To evaluate olfaction in mice, the buried food test was used as previously described (Yang and Crawley, 2009) with some modifications. Briefly, 7-week-old mice from each experimental group were fasted for 24 hours before the test. Next, the mice were individually habituated for 10 minutes in a new cage with fresh bedding. During the habituation step, a piece of standard chow (1×1 cm) was buried under the bedding in the middle of new cage (test cage) to a depth of 0.5 cm. The subject was then placed in the left corner of the test cage and allowed to move freely to seek the hidden food for 3 minutes. During this time, all activities, including sniffling around or digging in the bedding, was recorded until the mouse discovered the food and began to eat (latency). If

the mouse was unable to locate the food within 3 minutes, the result was categorized as a 'failure' (Figs. 15B and 20B) and was also excluded from the mean latency calculations (Figs. 15C and 20C). Directly after the test, each mouse underwent another trial with the food placed on top of the bedding (exposed food test) to ensure that the buried food test was based on olfaction and not on visual ability.

(3) Cyclosporin A (CsA) administration

Chronic microglial inhibition was conducted by CsA treatment (Chong Kun Dang, South Korea), a broad anti-inflammatory drug. Four-week old NPC1 mice were injected with CsA (5 mg/kg, prepared in normal saline) every second day for 4 weeks and the control group received the same volume of normal saline without CsA.

(4) 5-Bromo-2'-deoxyuridine (BrdU) administration

To trace the fate of proliferating cells in the OB, 4-week-old mice received a single injection of BrdU (Sigma-Aldrich, St. Louis, MO) (50 mg/kg, dissolved in 0.9% NaCl) intraperitoneally (i.p) and sacrificed after one month. Meanwhile, the short-term characterization of proliferating cells was achieved by a BrdU injection (100 mg/kg, i.p) into 4- or 8-week-old mice 4 or 24 hours before the euthanasia. The control subjects received the same volume of normal saline.

(5) Tissue processing

Tissue preparation was performed as previously described (Seo et al., 2011). For

RNA and protein extraction, mice were sacrificed by cervical dislocation, and whole brains were immediately collected. Then, OBs were collected for homogenization with Trizol (Invitrogen, Carlsbad, CA) (for RNA) or lysis buffer (Pro-prep; Intron Biotechnology, Korea) (for protein) using a TissueLyser II (Qiagen, Valencia, CA). For immunohistochemistry, mice were perfused with normal saline and then with 4% paraformaldehyde for 20 minutes each. The isolated whole brains containing OBs were post-fixed in 4% paraformaldehyde another 24 hours and transferred to a 30% sucrose solution for 3-4 days until they sank. In some experiments, the OE was also isolated after perfusion and immersed in a 0.5 M EDTA/10% sucrose solution for decalcification. Tissues were then placed into a mold filled with infiltration mixture (OCT compound) (Sakura Finetek, Japan) and stored at -80 °C until processing for cryosections.

(6) Quantitative real time-PCR (qRT-PCR) based gene expression analysis

RNA quantification and Reverse transcription PCR were performed as previously described (Seo et al., 2011). qRT-PCR was performed by mixing cDNA with primers and SYBR Green PCR Master Mix (Applied Biosystems, Foster City, CA) using an ABI 7500 Real time-PCR System with the supplied software (Applied Biosystems) according to the manufacturer's instruction. The primer sequences used in this study were as follows: Tumor necrosis factor-α (TNF-α), Forward 5'-AGGCTGTGCATTGCACCTCA-3' and Reverse 5'-GGGACAGTGACCTGGACTGT-3'; Interleukin-1β (IL-1β), Forward 5'-GATCCACACTCTCCAGCTGCA-3' and Reverse 5'-CAACCAACAAGTGATATTC-TCCAT-3'; IL-6, Forward 5'-AAGTGCATCATCGTTGTTCATACA-3' and Reverse 5'-

GAGGATACCACTCCCAACAGACC-3'; and Arginase 1 (Arg1), Forward 5'-GAACACGGCAGTGGCTTTAAC-3' and Reverse 5'-TGCTTAGCTCTGTCTGCTTTG-C-3'. Each relative mRNA level was calculated using the comparative Ct method and then normalized to Glyceraldehyde 3-phosphate dehydrogenase (Gapdh) mRNA levels.

(7) Western blot analysis

Protein quantification and western blot analysis were performed as previously described (Seo et al., 2011). Equal amounts of each protein sample were loaded onto 8-15 % SDS-PAGE gels and then transferred to a nitrocellulose membrane for standard blocking with bovine albumin serum followed by incubating with primary antibodies. The following primary antibodies were used: Olfactory marker protein (OMP) (1:500; Osenses, Australia), Glutamate decarboxylase 65 (GAD65) (1:1000; Abcam, Cambridge, MA), Tyrosine hydroxylase (TH) (1:1000; Millipore, Billerica, MA), Calbindin (CBD) (1:1000; Millipore), Doublecortin (DCX) (1:1000; Millipore) and Gapdh (1:2000; Millipore). Blots were developed with peroxidase-conjugated secondary antibodies (1:5000; Zymed Laboratories Inc., San Francisco, CA) and enhanced-chemiluminescence reagents (Intron Biotechnology). The relative band density was determined using Image J software (version 1.42q, NIH).

(8) Immunohistochemistry

The nasal cavity sections (12-μm thick) or whole brain sections (30-μm thick) were washed with PBS to remove the OCT compound. Sections were blocked with 5%

normal goat serum in PBS and then transferred to a primary antibody solution. The following primary antibodies were used: OMP (1:1000; Osenses), Iba1 (1:500; Wako, Japan), GAP43 (1:500), GAD65 (1:500), BrdU (1:250), and Ki67 (1:250) (all from Abcam); and TH, CBD, DCX and Neuronal nuclei (NeuN) (1:1000; all from Millipore). To detect BrdU- and Ki67-positive cells, sections were pre-treated with 2 N hydrochloric acid for 30 minutes at 37 °C to denature the DNA strands and then neutralized in 0.1 M borate buffer before the blocking step. Primary antibodies and cell nuclei were detected with appropriate Alexa 488- or 594-conjugated secondary antibodies (1:1000; Molecular Probes, Eugene, OR) and 4',6-diamidino-2-dhenylindole dihydrochloride (DAPI) (Zymed Laboratories Inc.), respectively. Images were captured with an Eclipse TE200 confocal microscope (Nikon, Japan), and additional histological analysis followed. No specific immunoreactivity was observed when the primary or secondary antibodies were omitted.

(9) Determination of region of interests (ROIs) and histological analysis

Consecutive coronal sections (spaced 180 μm apart) containing the SVZ were collected to assess the number of proliferating cells in the SVZ. All BrdU-incorporated cells within the lateral wall of the SVZ were counted. For histological analysis of the OB, 5 to 6 alternative representative sagittal sections of the main olfactory bulb region (500-800 μm lateral to the midline of the left hemisphere) were selected, and the entire region, including the glomerular and granule cell layers, was captured as shown in Fig. 2A. A total of 8 to 10 appropriate nasal cavity sections per animal were selected according to the turbinate structure, and each section contained 3 ROIs in the septum, endoturbinate II and

ectoturbinate 2, which was specified as the space between the epithelial surface and basal lamina (described in Fig. 16B). Cell counting results are expressed as the average number of immuno-labeled cells per mm^2. To determine relative immunoreactivity, the density of each positive signal within the ROI was measured using NIH Image J software version 1.63, and the WT value was set at 100%. All analytical procedures were conducted by a researcher blinded to the experimental conditions, and all experiments used sections that were carefully matched anatomically between animals.

(10) OB flow cytometry analysis

To analyze the microglial population in WT and NPC1-OB mice, 8-week old mice were euthanized, and the OB were immediately removed for the tissue dissociation with a Papain/DNase I solution for 45 minutes at 37 °C. After filtration through a strainer, cells were incubated with CD11b, CD86 or CD206 antibodies (all from Abcam). The cells expressing with each marker were detected with an Alexa 488 secondary antibody (Molecular Probes) and were analyzed for fluorescence on a FACS Caliber (Becton Dickinson, Franklin Lakes, NJ, USA).

(11) Statistical analysis

All data are expressed as the mean ± SEM from independent experiments. For statistical comparisons, Student's t-test and one-way ANOVA with a Bonferroni post-hoc analysis were performed using GraphPad Prism (v5.0, GraphPad), and differences were considered significant at $P < 0.05$.

2.3 RESULTS

(1) Olfactory impairment in NPC1 mice

Recently, Hovakimyan *et al.* reported neural defects in the OE and OB of an NPC1 model (Hovakimyan et al., 2013). Because axodendritic synaptic activity between the OE and OB is important in olfactory information processing (Lledo et al., 2005), I hypothesized that NPC1 mice would exhibit olfactory functional deficits. To confirm this hypothesis, I conducted a buried food pellet assay and recorded the latency to discover and begin eating the hidden food (Fig. 15A). Mice were assessed at 7 weeks of age (representative of a symptomatic stage), and all subjects showed normal locomotion during this test. Remarkably, NPC1 mutants (n= 17) performed the test less efficiently than WT mice (n= 20), and 41% of the NPC1 mice failed to find the pellet within the 3 minute cut-off time, but all WT mice successfully completed the test (Fig. 15B). On average, WT mice required approximately 55 seconds to find the food, and the majority of them (65%) began to eat the food within one minute (Figs. 15B and 15C). In contrast, the average latency for NPC1 mice to find the hidden pellet (n= 10, excluding failed attempts) was approximately 114 seconds (Fig. 15C). Considering that neither WT nor NPC1 mice had difficulty locating the exposed food (Fig. 15D), my findings indicate that olfaction is impaired in NPC1 mice.

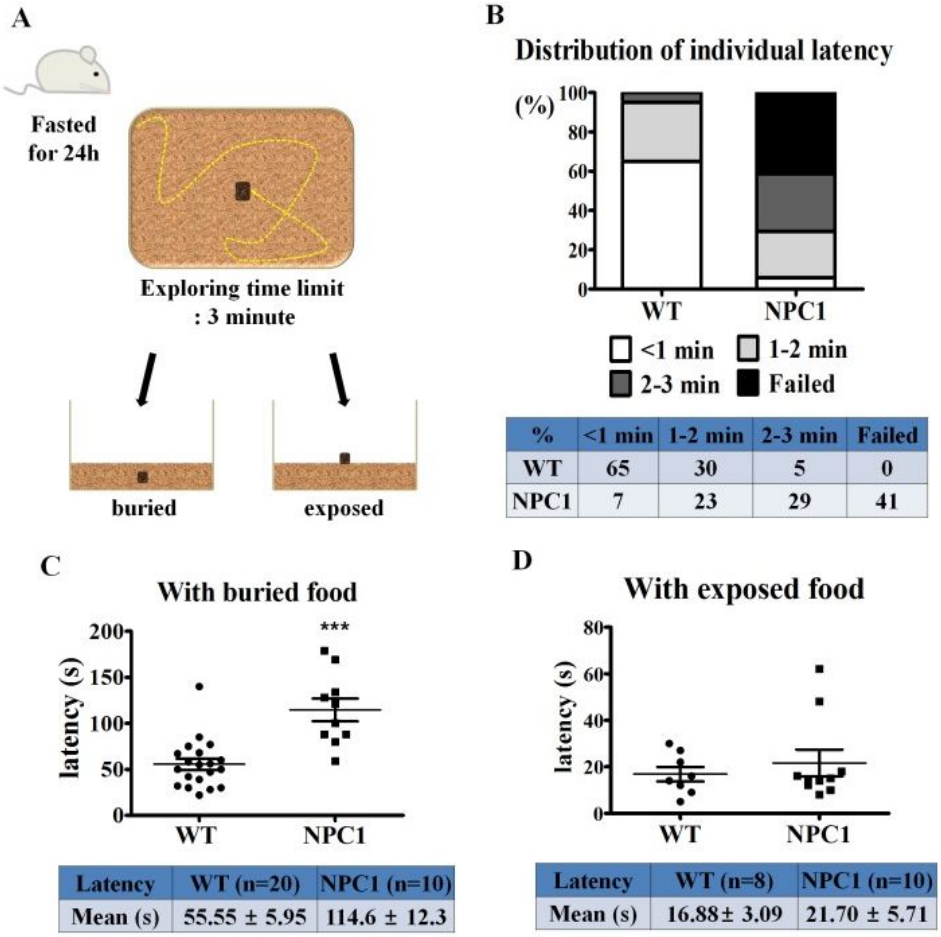

%	<1 min	1-2 min	2-3 min	Failed
WT	65	30	5	0
NPC1	7	23	29	41

Latency	WT (n=20)	NPC1 (n=10)
Mean (s)	55.55 ± 5.95	114.6 ± 12.3

Latency	WT (n=8)	NPC1 (n=10)
Mean (s)	16.88± 3.09	21.70 ± 5.71

Figure 15. Performance of WT and NPC1 mice on buried or exposed food finding tests.

(A) The experimental test design. (B) Individual latencies of WT (n=20) and NPC1 mice (n=17) to recover the buried food are shown as stacked bar graphs. Seven NPC1 mutants failed to locate the food. (C and D) Mean latencies with buried (C) or exposed food (D). On average, NPC1 mice (n=10) spent almost twice as much time finding the hidden food as WT mice (n=20). Failures (WT: none; NPC1: n=7) were excluded from the calculation. All data represent the mean ± SEM. ***P < 0.001.

(2) OSN degeneration in the OB of NPC1 mice (NPC1-OB)

I visualized neuronal distribution patterns in the OE and OB using immunohistochemistry, which assessed the impact of NPC1 dysfunction on olfactory structures. As previously described (Hovakimyan et al., 2013), a considerable reduction in axonal inputs of the OSNs (OMP^+ cells) towards the OB was detected in 8 week-old NPC1 mice compared with WT mice (Fig. 16A). I next examined the neuronal precursor population within the OE, which is responsible for OSN regeneration, and found that the immature neuronal pool ($GAP43^+$ cells) was reduced in the NPC1-OE compared with the WT-OE (Figs. 16B and C). Moreover, anti-TH reactivity of periglomerular neurons in the glomerular layer (GL) of the OB was noticeably decreased in NPC1 mice (Fig. 16D), and immunoblotting analysis of OB proteins extracted from 8 week-old mice confirmed my histological findings (Fig. 16E).

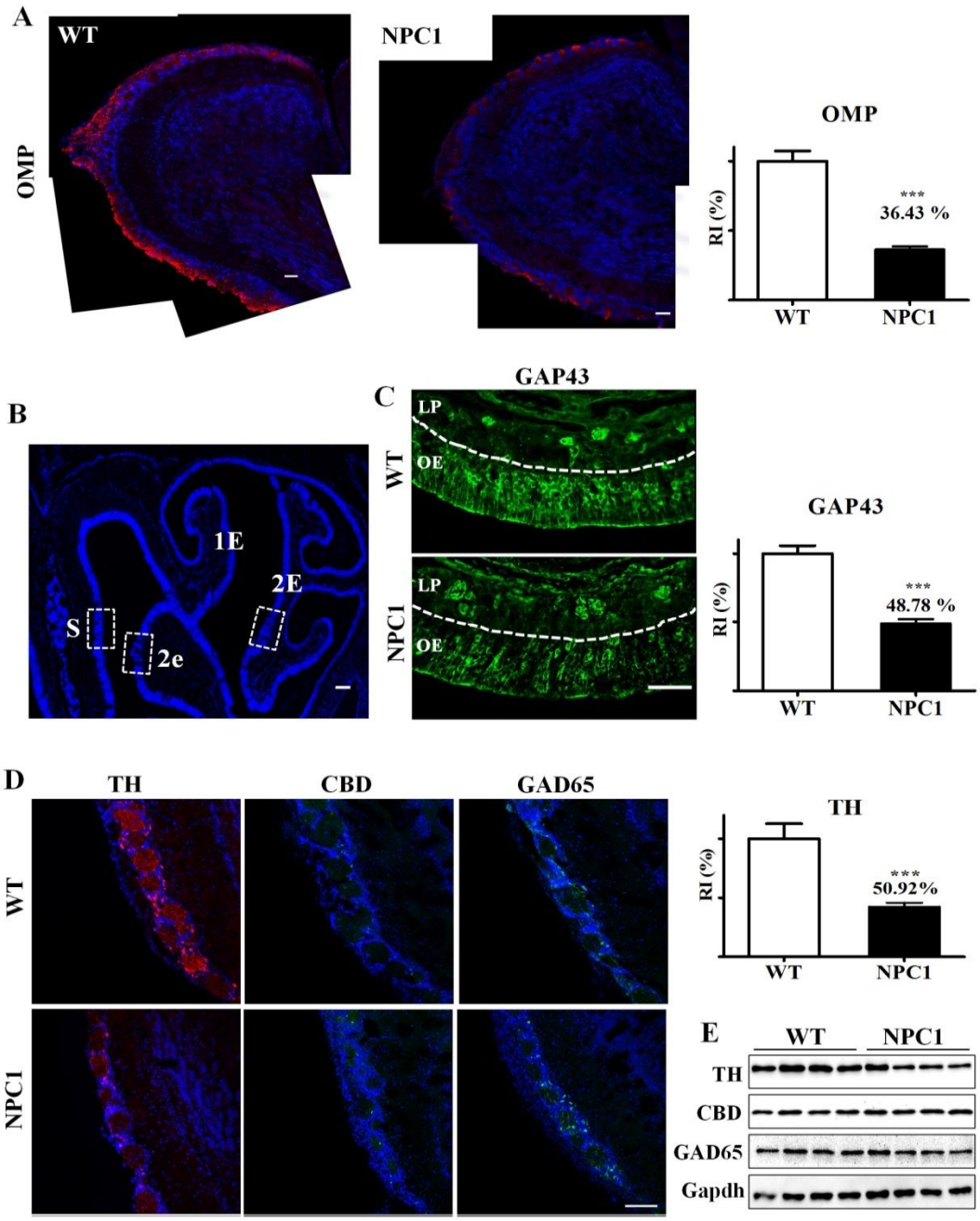

Figure 16. OSNs and other neuron distribution patterns in the OE and OB.

(A–D) Representative immunofluorescent images of the distribution patterns of OSNs

(OMP+) towards the OB (A), immature neurons in the OE ($GAP43^{+}$) (C) and various PG neurons expressing TH, CBD and GAD65 in the OB (D) are shown. The relative immunoreactivity (RI) of OMP (A), GAP43 (C) and TH (D) in the NPC1 samples is presented as the percentage of WT immunoreactivity. In the nasal cavity sections, 3 ROIs (S: septum; 2E: ectoturbinate 2; 2e: endoturbinate) were selected according to the turbinate structure as indicated in (B). (E) Western blots of neuronal proteins in the whole OBs extracted from the 8-week-oldmice support the immunohistochemical data. A total of 4 and 3 images were merged to complete the entire OB images of WT and NPC1mice, respectively, in (A). Scale bars = 100 μm (A, B and D); 50 μm (C). All data represent the mean ± SEM. ***P < 0.001.

(3) A decline in neuronal survival in the NPC1-OB

Odor input from OSNs in the OE is further processed in the OB through reciprocal neuronal actions (Shipley and Ennis, 1996). The majority of OB neurons are local granule neurons that refine incoming signals, and they are continuously replenished by subventricular zone (SVZ)-derived newborn cells throughout life (Breton-Provencher and Saghatelyan, 2012). To evaluate the capacity of neuronal turnover in the OB, I investigated the distribution pattern of neuroblasts in the OB using immunofluorescent staining for DCX, a neural precursor marker. As shown in Figs. 17A and B, a significant reduction in DCX immunoreactivity was observed in the OB of 8-week-old NPC1 mutants, which suggests that the production of neuroblasts in the SVZ and/or the survival of newborn neurons are defective in the SVZ-OB axis of NPC1 mice. Next, I used a BrdU tracking technique to clarify the cause of neuroblast loss in the NPC1-OB. NPC1 and WT mice received a BrdU injection at 4 or 8 weeks of age and were sacrificed after 24 hours to label the proliferative cell population in the SVZ, and some of the 4 week-old subjects were analyzed 4 weeks later to evaluate the survival rate of newborn cells in the OB. Interestingly, no significant differences were observed in the BrdU incorporation rate of newborn SVZ cells after a 24-hour BrdU pulse between NPC1 and WT mice at both 4 and 8 weeks of age, which implies that the proliferative capacity of neural precursor cells in the SVZ is primarily intact in NPC1 mice even during late disease stages (Figs. 17C and D). Four weeks after a BrdU injection, however, the number of newly generated mature OB neurons (NeuN/BrdU double-positive cells) labeled at 4 weeks of age in NPC1 mice was reduced by approximately 50% compared with WT mice (Fig. 17E).

Further immunohistochemical analysis revealed an increase in the number of cells undergoing apoptosis (activated caspase 3-positive cells) in the NPC1-OB (Fig. 17F). Therefore, my data suggest that a decreased newborn neuronal survival rate is responsible for the loss of neuroblasts, which ultimately impedes proper neuronal turnover in the OB of NPC1 mice.

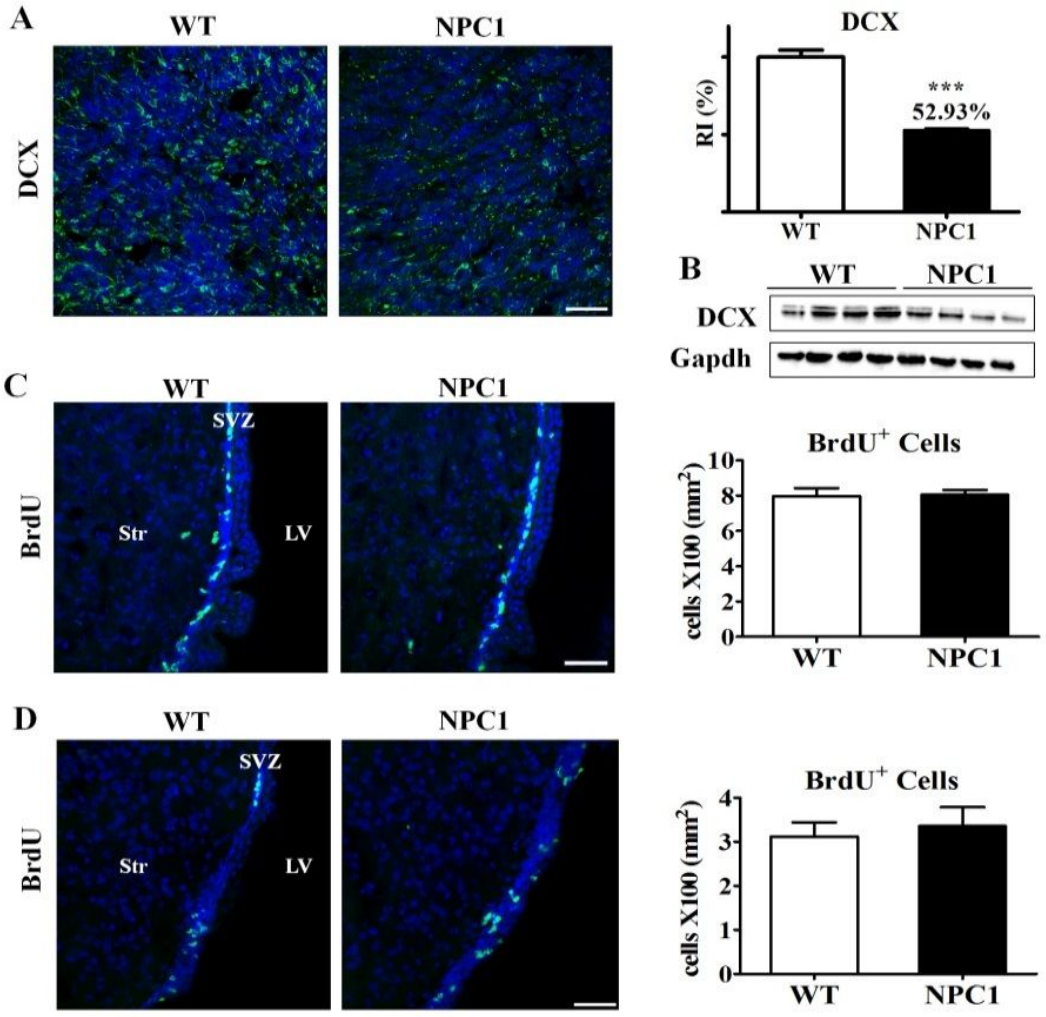

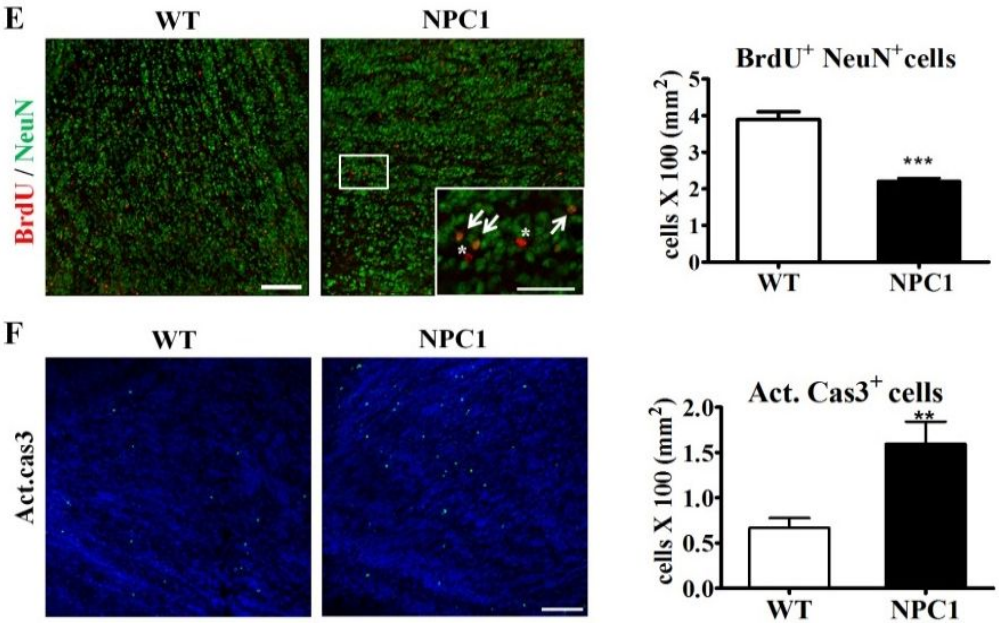

Figure 17. Decreased neuroblasts and neuronal survival in the NPC1-OB.

(A) Immunohistochemical images of neuroblasts (DCX^+) and RI quantification of the DCX-positive area of the WT- and NPC1-OB at 8 weeks of age. (B) Indirect quantification of the neuroblast population by Western blotting also implies decreased neurogenesis in the 8 week-old NPC1-OB. (C and D) To evaluate the on-going neurogenic activity in the SVZ, 24 h of BrdU cell tracking was conducted in WT and NPC1 mice at 4 weeks (C) or 8 weeks (D) of age. The total number of BrdU incorporated cells in the SVZ was not affected by NPC1 dysfunction. (E) The fate of SVZ-derived newborns was traced with BrdU for 4 weeks and analyzed using immunohistochemistry. $BrdU^+$ cells and $BrdU^+/NeuN^+$ cells are indicated by asterisks and arrows, respectively. (F) Representative confocal images indicating apoptotic cells ($Act.cas3^+$) in the WT- and NPC1-OB. Scale bars = 50 μm (A, C, D, E and F); 10 μm (magnified square images in E). All data represent the mean ± SEM. $^{**}P < 0.01$ and $^{***}P < 0.001$.

(4) Abnormal microgliosis is highly activated in the NPC1-OB

Because NPC1 progression is accompanied by enhanced inflammation (Baudry et al., 2003), I next examined the number and activation state of microglia in the WT- and NPC1-OB using Iba1 immunostaining. At 4 and 8 weeks of age, NPC1 mice showed a remarkable increase in the total number of microglial cells in the glomerular layer (GL) and granule cell layer (GCL) (ratio to WT control: 1.8 at 4 weeks and 2.21 at 8 weeks in the GCL; 1.38 at 4 weeks and 1.84 at 8 weeks in the GL, $P < 0.001$) (Figs. 18A-C). I also found that amoeboid-like reactive microglia accounted for a significant portion of the total $Iba1^+$ cell population in the NPC1-OB, whereas the majority of $Iba1^+$ cells in the WT-OB were in a resting state (Figs. 18A' and 18A"). Thus, I distinguished the phenotype of activated microglia within the OB between M1 (pro-inflammatory) and M2 (anti-inflammatory) types based on signature gene expression patterns using real-time PCR. I observed that the gene expression levels of IL-1β and TNF-α, which were used as representative genes for the M1 type microglia, were significantly elevated in the NPC1-OB at 8 weeks of age, but the expression of the M2 marker Arg1 was similar in WT and NPC1 mice (Fig. 18D). Flow cytometry analysis of the entire microglial population within the OB confirmed these observations. Most NPC1-derived microglia were labeled with a CD86 marker, indicating a M1 microglial phenotype, but some cells were identified as $CD206^+$, a M2 microglial phenotype marker (Fig. 18E). Overall, these data clearly demonstrate that the abnormal neurotoxic activation of microglia occurs in the NPC1-OB.

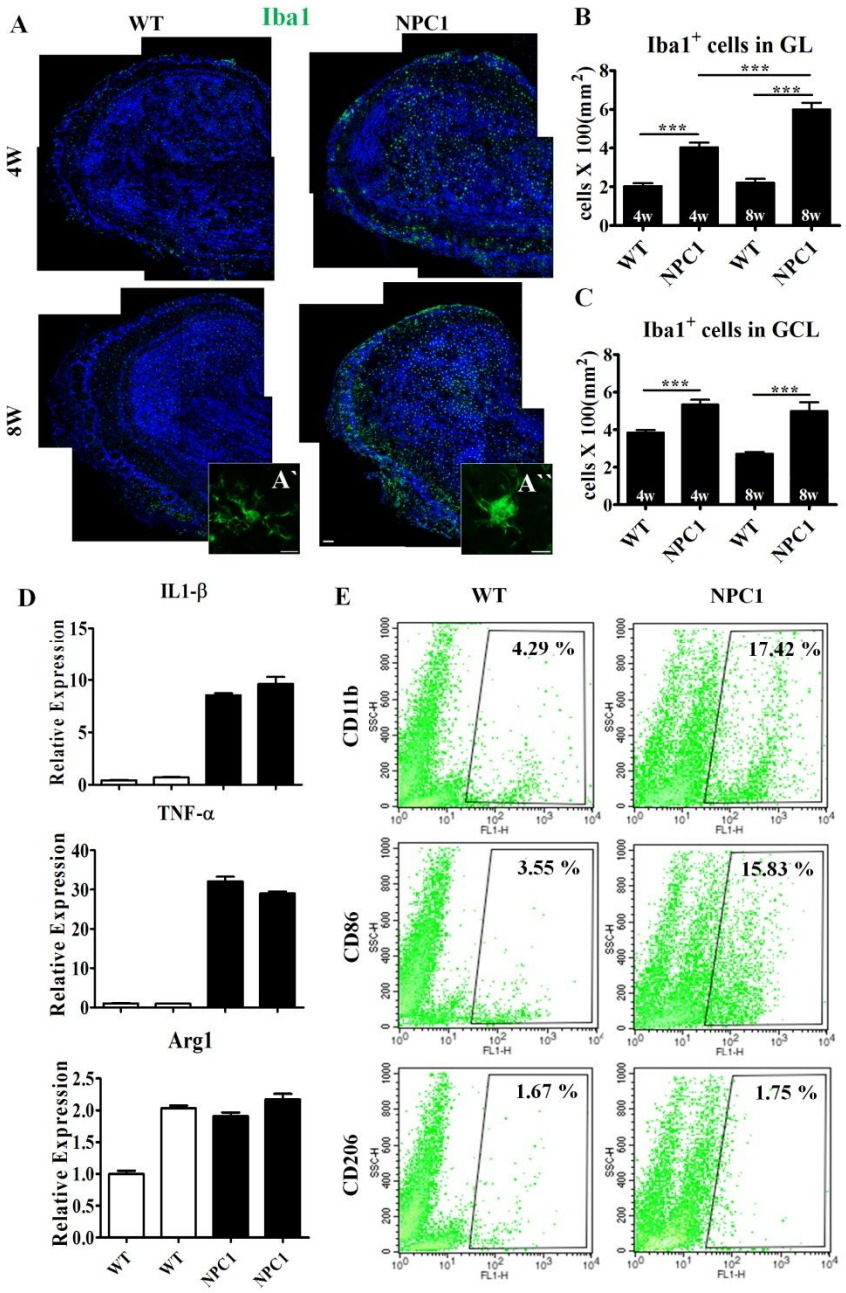

Figure 18. Neurotoxic (M1 type) microglia accumulation in the NPC1-OB.

(A) The distribution patterns of microglia in the OB are visualized using Iba1

immunohistochemistry. Representative magnified images of resting (A′) and activated (A″) are also shown. (B and C) The total number of Iba^+ cells in the GL (B) and GCL (C) was quantified. (D) mRNA expression analysis of the representative microglial activation markers, including IL-1, TNF-α, and Arg1 in the OB of WT and NPC1 mice (n=3 for each group), was performed by real-time PCR. Each sample was tested in triplicate, and one mean WT value (randomly chosen) was standardized as 1 for convenience. (E) For the characterization of microglial phenotypes in the WT- and NPC1-OB, dissociated microglia were conjugated with CD11b (pan-microglial marker), CD86 (M1 marker) and CD206 (M2marker) and analyzed using flow cytometry. Four images were merged to complete the entire OB images of WT and NPC1 mice in (A). Scale bars=100 μm(A); 10 μm(A′ and A″). All data represent the mean ± SEM. ***P b 0.001.

(5) Disrupted neuronal integrity with enhanced microgliosis in the NPC1-OB

Next, I conducted an *in vivo* BrdU cell tracking assay to quantitate on-going microgliosis. Four week-old NPC1 and WT animals received a single intraperitoneal BrdU injection 4 hours before perfusion to detect the rapidly proliferating cell population, which would be largely microglia. Immunohistochemical analysis revealed that the majority of $BrdU^+$ cells (>90%) within the OB were co-immunostained with Iba1, as expected (Fig. 19A). Importantly, the number of BrdU/Iba1 double-positive cells in NPC1 mutants was significantly increased, by more than seven-fold, compared with WT controls, implying the presence of extensive microgliosis in the NPC1-OB (Fig. 19A).

I further investigated the total amount of accumulated microglial cells in the NPC1-OB using a 4 week-long BrdU cell tracking technique, as described in 3.2 section. Immunohistochemical analysis revealed that the total number of $BrdU^+/Iba1^+$ cells in the NPC1-OB was approximately three-fold higher compared with the WT control (Fig. 19B). In the WT-GCL, approximately 80% and 10% of $BrdU^+$ cells differentiated into $NeuN^+$ mature neurons and $Iba1^+$ microglia, respectively (Fig. 19C). In the mutant GCL, however, only half of the BrdU incorporated cells expressed NeuN, whereas $Iba1^+$ cells accounted for over 30% of the newly generated cells (Fig. 19C). Therefore, I infer that olfactory deficits are related to the presence of persistent reactive microgliosis and decreased neuronal turnover in the OB of NPC1 mice.

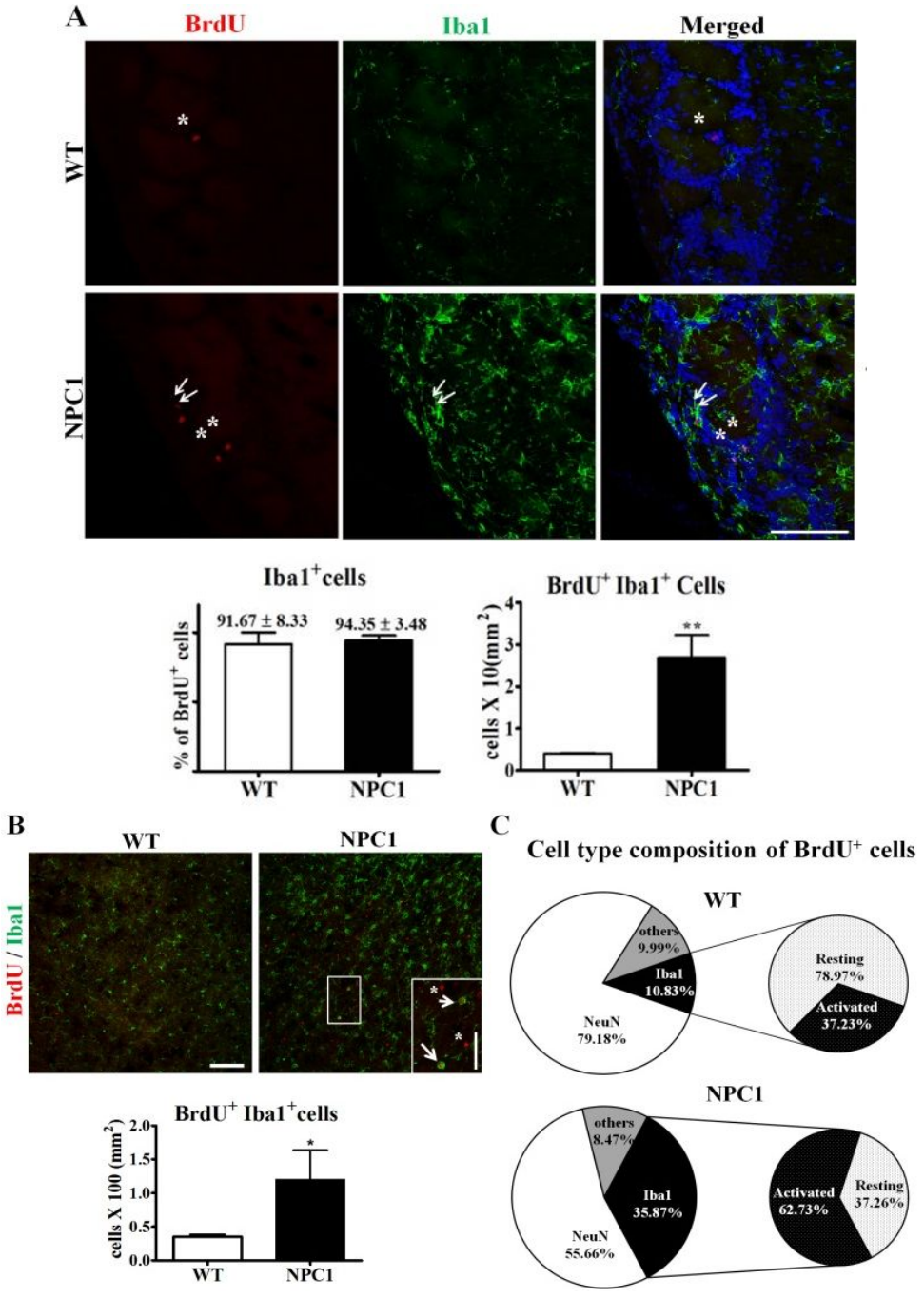

Figure 19. Reactive microgliosis in the NPC1-OB.

(A) In the representative confocal images, $BrdU^+$ cells and $BrdU^+/Iba^+$ cells (rapid

proliferating microglia) are indicated by asterisks and arrows, respectively. (B and C) Four-week-old WT and NPC1 mice received a BrdU injection and were sacrificed 4 weeks later for long-term newborn cell tracking. $BrdU^+$ cells and $BrdU^+/Iba^+$ cells are indicated by asterisks and arrows, respectively. Scale bars = 50 μm (A and B); 10 μm (magnified square images in B). All data represent the mean ± SEM. *$P < 0.05$ and **$P < 0.01$.

(6) Microglial inhibition with Cyclosporin A (CsA) improves olfaction in NPC1 mice

I decided to suppress microglial activity in the NPC1-OB with CsA, a powerful immunosuppressant, to evaluate its therapeutic potential to restore olfaction. NPC1 mice received CsA (n=19) or normal saline (n=22) injections (i.p) for a total of 4 weeks beginning at 4 weeks of age, and then microglial activity in the NPC1-OB was examined using immunocytochemistry. I found that a 4-week-long CsA treatment significantly reduced the number of OX-42^{+} cells, which represent activated microglia, throughout the NPC1-OB (Fig. 20A). Next, I performed the buried food test with all subjects at 7 weeks of age to determine whether CsA improved olfactory dysfunction in NPC1 mice. Continuous CsA injections contributed to an overall improvement in the olfaction of NPC1 mice, but it had no effect on olfactory performance of WT mice (Figs. 20B and C). Indeed, the mean latency of saline-injected NPC1 mice did not differ from the untreated NPC1 mice shown in Figure 15; however, NPC1 mice treated with CsA showed a tendency to find pellets faster than the controls (Figs. 20B and C).

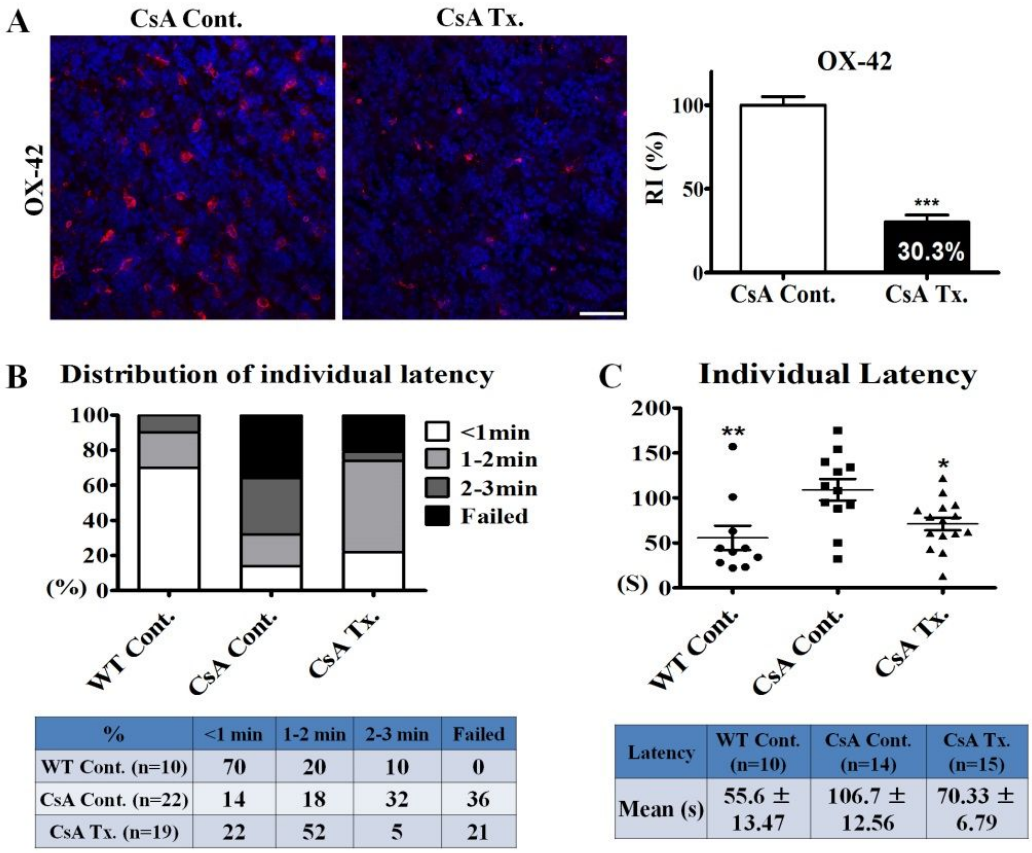

%	<1 min	1-2 min	2-3 min	Failed
WT Cont. (n=10)	70	20	10	0
CsA Cont. (n=22)	14	18	32	36
CsA Tx. (n=19)	22	52	5	21

Latency	WT Cont. (n=10)	CsA Cont. (n=14)	CsA Tx. (n=15)
Mean (s)	55.6 ± 13.47	106.7 ± 12.56	70.33 ± 6.79

Figure 20. CsA treatment inhibits microgliosis and reduces olfactory impairment.

To suppress microglial activation, CsA was injected every other day for one month in 4-week old mice. (A)OX-42 immunostaining and its density analysis show that CsA administration could inhibit extensive microgliosis in the NPC1-OB. (B and C) CsA-treated NPC1 mice (CsA Tx., n = 19) show improved performances in the buried food test compared with the normal saline treated group (CsA Cont., n = 22). Failures (CsA Tx.: n = 4; CsA Cont.: n= 8) were excluded from the calculation for (C). Continuous injection of CsA had no effect on the olfactory performance of WT mice (WT Cont.: n= 10). Scale bars = 50 μm (A). All data represent the mean ± SEM. *P < 0.05, **P < 0.01, and ***P < 0.001.

The amelioration of olfactory dysfunction in CsA-treated NPC1 mice may be due to the protection of OE or OB neurons by attenuated microgliosis. Notably, CsA administration slightly increased both the intensity of GAP43-positive areas within the OE (Fig. 21A) and OMP expression levels in the OB (Fig. 21B). However, the protection of neural precursor cells and OSNs in the NPC1-OE might not be sufficient to explain the role of microglial inhibition in improving olfactory dysfunction because the OMP intensity in the CsA-treated NPC1-OB was approximately 50% of the WT-OB (Fig. 21B). Conversely, continuous CsA injections readily increased the total number of DCX^+ cells by approximately 66% in the GL (Fig. 21C). To understand the cause of this cellular increase, I first labeled proliferating cells with BrdU for 24 hours on the last day of CsA or normal saline treatment and compared the SVZ neurogenic capacity in CsA-treated and control NPC1 mice. No difference in the number of BrdU-positive cells was observed between the two groups, indicating that the proliferation of neural stem/progenitor cells was not affected by CsA treatment (Fig. 21D). I then investigated whether microglial inhibition provided the positive effect on neuronal survival followed by an expansion of the neuronal pool in the NPC1-OB. Thus, NPC1 mice received a single BrdU injection on the first day of CsA or normal saline administration, and $BrdU^+$ cells were further stained 4 weeks later for the expression of the neuronal marker NeuN. The fraction of BrdU incorporated cells derived from the SVZ that gave rise to mature granule neurons in the GCL increased approximately 1.5-fold in the CsA-treated NPC1-OB compared with normal saline controls (Fig. 21E). Moreover, the proportion of apoptotic neurons decreased after CsA administration (Fig. 21F), implying that excessive microglial activity is related to the loss of interneurons in the NPC1-OB.

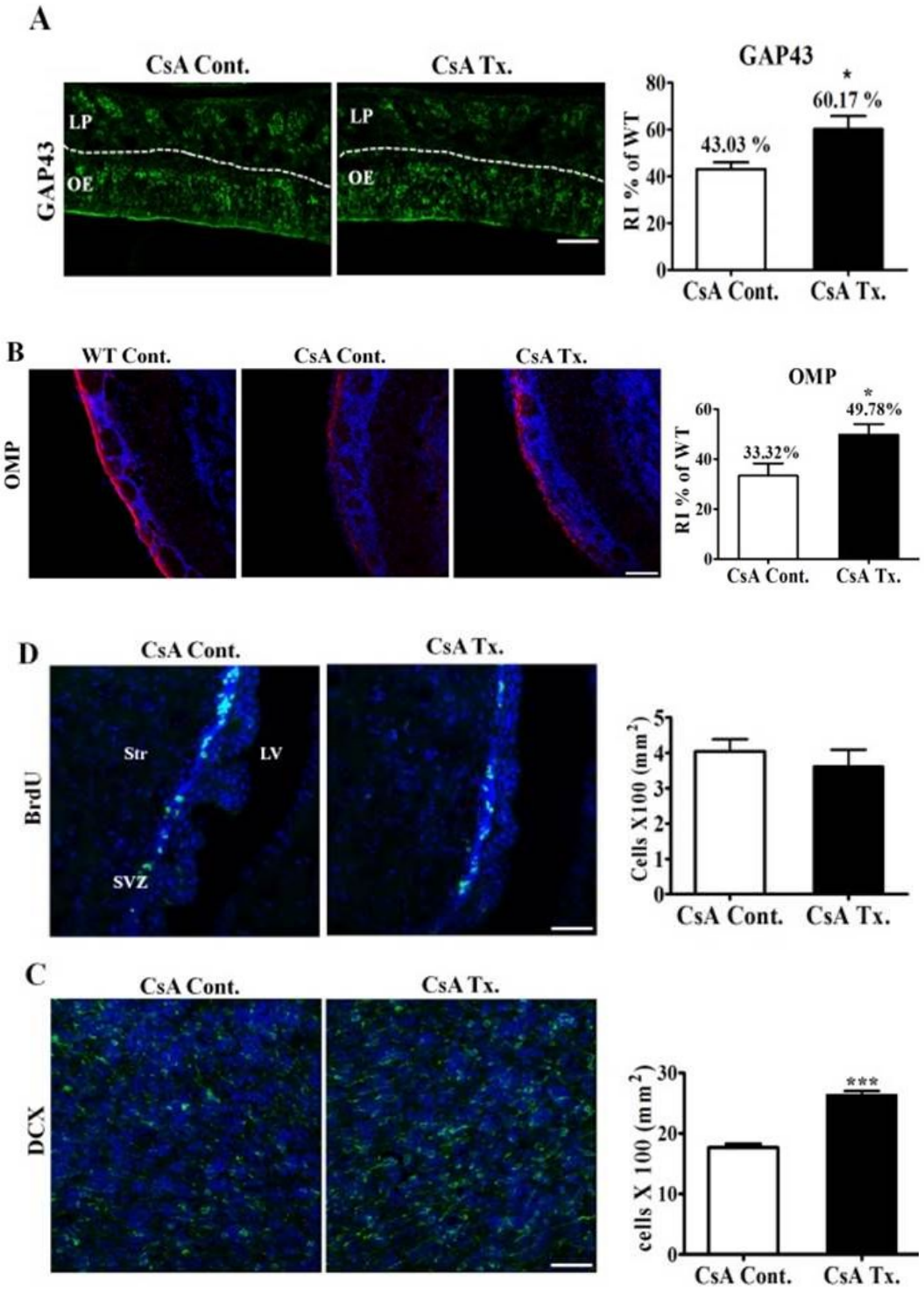
A
CsA Cont.
CsA Tx.
GAP43
LP
OE
GAP43
RI % of WT
43.03 %
60.17 %
*
CsA Cont.
CsA Tx.
B
WT Cont.
CsA Cont.
CsA Tx.
OMP
OMP
RI % of WT
33.32%
49.78%
*
CsA Cont.
CsA Tx.
D
CsA Cont.
CsA Tx.
BrdU
Str
LV
SVZ
Cells X100 (mm2)
CsA Cont.
CsA Tx.
C
CsA Cont.
CsA Tx.
DCX
cells X 100 (mm2)
***
CsA Cont.
CsA Tx.

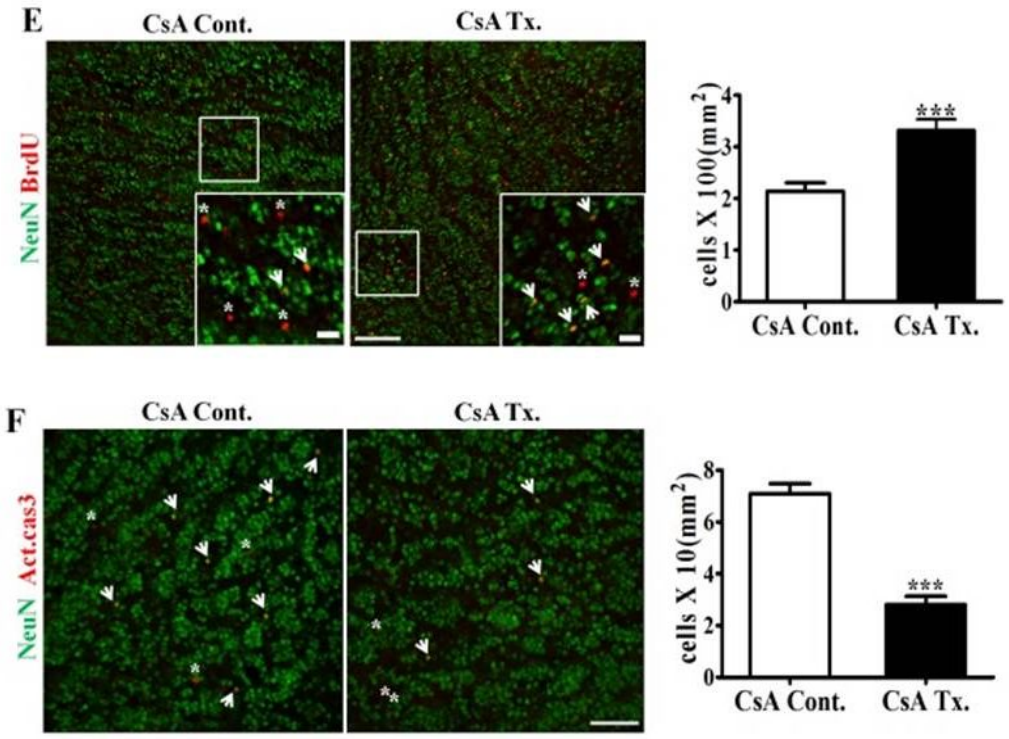

Figure 21. Microglial inhibition improves newly generated neuron survival.

(A, B, C) Representative OE and OB images of GAP43 (A), OMP (B) and DCX (C) in NPC1 mice after a 4-week administration of normal saline or CsA. (D) A 24h BrdU pulse in 4-week-old mice revealed that neurogenic activity in the SVZ was not altered by suppression of microglial activity. (E) Immunohistochemistry of newly generated mature neurons ($BrdU^+/NeuN^+$) in the control- and CsA-treated NPC1-OB demonstrate the beneficial effects of microglial inhibition on neurogenesis. $BrdU^+$ cells and $BrdU^+/NeuN^+$ cells are indicated by asterisks and arrows, respectively. (F) To detect apoptotic OB neurons, immunofluorescent double labeling of activated caspase 3 (Act.cas3) and NeuN was conducted. $Act.cas3^+$ cells and $Act.cas3^+/NeuN^+$cells are indicated by asterisks and arrows, respectively. Scale bars=50 μm (A, B, C, D, E and F); 10 μm (magnified square images in E). All data represent the mean±SEM. *P < 0.05, **P <0.01, ***P < 0.001.

2.4 DISCUSSION

Olfactory dysfunction has been considered as an important determinant of neurodegeneration because it precedes other neurological symptoms during the neurodegenerative process. In this study, I elucidated the role of excessive microglial activation, an often observed phenomenon in the damaged brain, in olfactory impairment using an NPC1 mouse model. Importantly, microglial accumulation in the OB reduced the population of OB interneurons by regulating the survival and apoptosis of granule neurons, which aggravates olfactory loss. Therefore, I suggest a causal relationship between microgliosis and olfactory impairment in neurodegeneration.

Mutations in the NPC1 genes lead to the systemic disruption of lipid trafficking. However, a pronounced neuropathology, such as tremor, ataxia and dementia, is one of the most important NPC1 features because it is ultimately responsible for most patient deaths (Vanier, 2010). Herein, I performed an olfactory behavior test that shows distinctive signs of olfactory impairment in NPC1 mice. Progressive neuronal loss in the olfactory complex of NPC1 mice is likely responsible for the deficit because I observed significant reductions in the pool of OSNs in NPC1 mice, as previously described (Hovakimyan et al., 2013). Interestingly, the over-expression of the amyloid precursor protein (APP) accelerates the synthesis of soluble Aβ and leads to aberrant axonal targeting and elimination of OSNs (Cao et al., 2012; Cheng et al., 2011). Considering that impaired lipid metabolism in NPC1 causes an abnormal processing of APP and Aβ

accumulation (Jin et al., 2004), it is possible that OSN loss is induced by APP- and Aβ-mediated cytotoxicity in NPC1 mice. In addition, based on my previous findings indicating that self-renewal and differentiation potency are impaired in neural stem cells in NPC1 mice both *in vitro* and *in vivo* (Kim et al., 2008; Yang et al., 2006), NPC1 mouse-derived olfactory stem cells might also have a defect in the regenerative capacity compared with WT cells. Although my present study reveals a reduced pool of OE-residing neuroblasts in NPC1 mutants, which may provide evidence for this hypothesis, further investigations focused on OE-related pathology are necessary to delineate the underlying mechanisms of OSN degeneration in NPC1 mice.

Postnatal microgliosis lasts for approximately 4 weeks in the rodent OB, then microglia gradually transform into a resting state and provide a constant surveillance system for the maintenance of normal brain functions (Fiske and Brunjes, 2000). However, my results suggest that persistent microgliosis develops in the NPC1-OB, which is also found in other brain regions (Baudry et al., 2003). Interestingly, the induction of TNF-α secretion after olfactory bulbectomy prevents the proliferation of OE neuroblasts and OSN regeneration and the following olfactory loss in mice (Pozharskaya et al., 2013; Turner et al., 2010). Therefore, the resolution of inflammation can be a key treatment strategy for olfactory dysfunction. In this context, I investigated the benefit of microglial inhibition to olfaction-related pathology in NPC1 mice. Similarly, microglial suppression using the anti-inflammatory agent CsA enhanced OSN regeneration by increasing the pool of neural progenitor cells in the NPC1-OE. However, the protective effects of CsA might be not enough to compensate for the loss of OSNs because the

axonal inputs of OSNs towards the NPC1-OB are still insufficient after CsA treatment when compared with the WT-OB. Thus, I suggest that microglial activity does not play a leading role in OSN degeneration in NPC1. My data support previous observations showing that neurodegeneration in NPC1 begins in neural cell-autonomous and microglial-independent manners (Peake et al., 2011). However, controlling microglial activity may be an important aspect of olfaction because microglial inhibition might positively influence the survival of interneurons in the SVZ-OB axis of NPC1 mice. These data are consistent with previous findings showing that neighboring microglia can alter neuronal network composition by regulating the neural precursor population in neurogenic centers through phagocytosis in intact and aged/diseased brains (Sierra et al., 2010; Vukovic et al., 2012). Microglia can also induce neural death by secreting neurotoxic molecules, such as reactive oxygen species or pro-inflammatory cytokines, especially in pathological situations (Block et al., 2007). Similarly, I revealed that subsequent microglial inhibition using CsA restored neuroblast survival and reduced the number of apoptotic granule neurons, proving the negative impact of massive microgliosis on the maintenance of the OB neuronal population.

The presence and physiological meaning of continuous neural replacement in the OB is under debate (Brus et al., 2013; Lazarini and Lledo, 2011). In most mammals, SVZ-derived neural precursor cells migrate through the rostral migratory stream to the OB, where they then differentiate into granule neurons (Breton-Provencher et al., 2009; Mouret et al., 2009; Nissant et al., 2009). Notably, normal olfactory function is disturbed by ablation of neurogenesis in mice infused with the antimitotic drug AraC (Breton-

Provencher et al., 2009) and in the neural cell adhesion molecule gene knock-out mice (Gheusi et al., 2000). These observations suggest the significance of neurogenic activity in the SVZ-OB axis in olfaction. However, no reliable evidence of neurogenic activity in the human SVZ has yet been uncovered (Brus et al., 2013), and Bergmann *et al.* have indicated that OB neurons exist from birth throughout life without replacement using C14 concentration analysis (Bergmann et al., 2012). Therefore, the loss of OB interneurons might be more critical in humans compared with other species because the maintenance of OB neuronal projections to other structures is important in olfaction (Lledo et al., 2008). In this respect, I infer that microglial activity would have a close relationship with the development of olfactory dysfunction during neurodegenerative processes in humans as well as in other species by regulating the survival of OB granule neurons. Indeed, I demonstrated that CsA treatment considerably reduced the number of mice that failed to locate the hidden food and decreased the latency to find the pellet. My data somewhat contrast a previous work that found minocycline-induced microglial inhibition had no effect on the recovery of olfactory dysfunction in a Dichlobenil-induced OB damage model (Lazarini et al., 2012). I speculate that these different outcomes of microglial inhibition may be attributed to the differences in olfactory damage between these two models. Dichlobenil induces acute necrosis within the olfactory mucosa accompanied by a severe reduction in the OSN population (Lazarini et al., 2012), whereas NPC1 dysfunction tends to cause a gradual OSN loss in a time-dependent manner. Therefore, the benefit of microglial inhibition might be insufficient to overcome the drastic olfactory impairment in the Dichlobenil-treated model. To confirm this hypothesis, it would be

worthwhile to determine the therapeutic effects of microglial inhibitors in a mildly damaged neurodegenerative model.

Overall, I emphasize the role of OB microglia in the development of olfactory dysfunction in NPC1 mice. Present microglial inhibition studies reveal that abnormal microgliosis may aggravate olfactory damage, creating the possibility of therapeutic applications for anti-inflammatory agents in patients with neurological disorders who exhibit olfactory impairment. My work also emphasizes the importance of bidirectional interactions between neurons and microglia in neurodegenerative processes.

GENERAL CONCLUSION

Niemann-Pick disease type C (NPC) is a fatal genetic disorder characterized by an impaired intracellular lipid trafficking system. Based on the fact that presence of neuropathy is regarded as crucial criteria to determine the prognosis of NPC-affected patient, my study has been focused on improving NPC-related neurological symptoms and elucidating its underlying mechanism using (1) transplantation of hUCB-MSCs and (2) immunosuppressant in the murine NPC1 model to suggest novel therapeutic approaches for the management of this incurable disease.

In the first study, I evaluated therapeutic potential of hUCB-MSCs transplantation in NPC neuropathy because MSCs from various tissues have been suggested as an alternative source for treatment of neurodegenerative diseases. The major expected benefits of stem cell application are known to replace damaged cells with themselves as well as to provide better microenvironment for endogenous cells by paracrine effects. Considering that hUCB-MSC transplantation promote the survival of Purkinje neurons and endogenous hippocampal neurogenesis with reduced glutamate-induced excitotoxicity and neuroinflammation in NPC1-affected mouse brain, I imply that hUCB-MSC can provide neuroprotection via producing considerable amounts of immune modulatory- and neurotrophic growth factors. It is also noted that a few of treated hUCB-MSCs had neuron-specific MAP2-positive signals in and around the transplanted site with an electrophysiological reaction *in vivo*, supportive to previous reports showing that

MSCs can be transdiffentiated into functional neurons. Ultimately, hUCB-MSCs improve motor function of NPC1 mice in Rota-rod behavior test and attenuated cholesterol accumulation in various brain regions.

In the second study, I decided to analyze the olfaction and OB-related neuropathology in NPC1-affected mice in the context that olfactory loss has been considered as an important earliest determinant of neurodegeneration, although the underlying mechanism for the dysfunction remains unclear. At 7 weeks of age, NPC1 mutants showed a distinct olfactory impairment in an olfactory test compared with age-matched WT. The marked loss of olfactory sensory neurons within the NPC1-OB suggests that NPC1 dysfunction impairs olfactory structure. Furthermore, the pool of neuroblasts in the OB was diminished in NPC1 mice despite the intact proliferative capacity of neural stem/progenitor cells in the subventricular zone. Instead, pro-inflammatory proliferating microglia accumulated extensively in the NPC1-OB as the disease progressed. To evaluate the impact of abnormal microglial activation on olfaction in NPC1 mice, a microglial inhibition study was performed using the anti-inflammatory agent CsA. Importantly, long-term CsA treatment in NPC1 mice reduced reactive microgliosis, restored the survival of newly generated neurons in the OB and improved overall performance on the olfactory test.

Therefore, these data suggests that hUCB-MSCs lead to several improvements in NPC1 mice, showing their potential as a therapeutic agent in neurodegenerative diseases. My study also provides a reasonable basis for the olfactory analysis of NPC patients and emphasizes the necessity of unravelling the role of microglia in the neurodegenerative

process of NPC1 to treat the disease. I anticipate that these findings would contribute to reveal the underlying basis of NPC1 pathology to understand complicated nature of NPC1-related neurodegenerative process and provide novel practical information in the fields of NPC1 therapeutics.

REFERENCES

Abi-Mosleh, L., Infante, R.E., Radhakrishnan, A., Goldstein, J.L., and Brown, M.S. (2009). Cyclodextrin overcomes deficient lysosome-to-endoplasmic reticulum transport of cholesterol in Niemann-Pick type C cells. P Natl Acad Sci USA *106*, 19316-19321.

Ajami, B., Bennett, J.L., Krieger, C., Tetzlaff, W., and Rossi, F.M.V. (2007). Local self-renewal can sustain CNS microglia maintenance and function throughout adult life. Nat Neurosci *10*, 1538-1543.

Albers, M.W., Tabert, M.H., and Devanand, D.P. (2006). Olfactory dysfunction as a predictor of neuro degenerative disease. Current neurology and neuroscience reports *6*, 379-386.

Ashwell, K. (1991). The distribution of microglia and cell-death in the fetal-rat forebrain. Dev Brain Res *58*, 1-12.

Bahar-Fuchs, A., Chetelat, G., Villemagne, V.L., Moss, S., Pike, K., Masters, C.L., Rowe, C.,Savage, G. (2010). Olfactory deficits and amyloid-beta burden in Alzheimer's disease, mild cognitive impairment, and healthy aging: a PiB PET study. Journal of Alzheimer's disease : JAD *22*, 1081-1087.

Baudry, M., Yao, Y., Simmons, D., Liu, J., and Bi, X. (2003). Postnatal development of inflammation in a murine model of Niemann-Pick type C disease: immunohistochemical observations of microglia and astroglia. Exp Neurol *184*, 887-903.

Beach, T.G., White, C.L., Hladik, C.L., Sabbagh, M.N., Connor, D.J., Shill, H. A., Sue, L. I.,Sasse, J., Bachalakuri, J., Henry-Watson, J., Akiyama, H., Adler, C. H. (2009).

Olfactory bulb α-synucleinopathy has high specificity and sensitivity for Lewy body disorders. Acta Neuropathol *117*, 169-174.

Bergmann, O., Liebl, J., Bernard, S., Alkass, K., Yeung, M.S.Y., Steier, P., Kutschera, W., Johnson, L., Landen, M., Druid, H., Spalding, K. L., Frisen, J. (2012). The Age of olfactory bulb neurons in humans. Neuron *74*, 634-639.

Beyer Nardi, N., and da Silva Meirelles, L. (2006). Mesenchymal stem cells: isolation, in vitro expansion and characterization. Handbook of experimental pharmacology, 249-282.

Blandini, F., Cova, L., Armentero, M.T., Zennaro, E., Levandis, G., Bossolasco, P., Bossolasco, P., Calzarossa, C., Mellone, M., Giuseppe, B., Deliliers, G. L., Polli, E., Nappi, G.,Silani, V. (2010) Transplantation of undifferentiated human mesenchymal stem cells protects against 6-hydroxydopamine neurotoxicity in the rat. Cell Transplant *19*, 203-217.

Block, M.L., Zecca, L., and Hong, J.S. (2007). Microglia-mediated neurotoxicity: uncovering the molecular mechanisms. Nature Reviews Neuroscience *8*, 57-69.

Bouchez, G., Sensebe, L., Vourc'h, P., Garreau, L., Bodard, S., Rico, A., Rico, A., Guilloteau, D., Charbord, P., Besnard, J. C., Chalon, S. (2008). Partial recovery of dopaminergic pathway after graft of adult mesenchymal stem cells in a rat model of Parkinson's disease. Neurochemistry International *52*, 1332-1342.

Breton-Provencher, V., Lemasson, M., Peralta, M.R., and Saghatelyan, A. (2009). Interneurons produced in adulthood are required for the normal functioning of the olfactory bulb network and for the execution of selected olfactory behaviors. J Neurosci *29*, 15245-15257.

Breton-Provencher, V., and Saghatelyan, A. (2012). Newborn neurons in the adult olfactory bulb: Unique properties for specific odor behavior. Behavioural brain research *227*, 480-489.

Brus, M., Keller, M., and Levy, F. (2013). Temporal features of adult neurogenesis: differences and similarities across mammalian species. Frontiers in neuroscience *7*, 135.

Burman, J., Iacobaeus, E., Svenningsson, A., Lycke, J., Gunnarsson, M., Nilsson, P., Vrethem, M., Fredrikson, S., Martin, C., Sandstedt, A., Uggla, B., Lenhoff, S., Johansson, J. E., Isaksson, C., Hagglund, H., Carlson, K., Fagius, J. (2014). Autologous haematopoietic stem cell transplantation for aggressive multiple sclerosis: the Swedish experience. Journal of neurology, neurosurgery, and psychiatry *85*, 1116-1121.

Byun, K., Kim, J., Cho, S.Y., Hutchinson, B., Yang, S.R., Kang, K.S., Cho, M., Hwang, K., Michikawa, M., Jeon, Y. W., Paik, Y. K., Lee, B. (2006). Alteration of the glutamate and GABA transporters in the hippocampus of the Niemann-Pick disease, type C mouse using proteomic analysis. Proteomics *6*, 1230-1236.

Cao, L.X., Schrank, B.R., Rodriguez, S., Benz, E.G., Moulia, T.W., Rickenbacher, G.T., Gomez, A. C., Levites, Y., Edwards, S. R., Golde, T. E., Hyman, B. T., Barnea, G., Albers, M. W. (2012). Aβ alters the connectivity of olfactory neurons in the absence of amyloid plaques in vivo. Nat Commun *3*.

Carstea, E.D., Morris, J.A., Coleman, K.G., Loftus, S.K., Zhang, D., Cummings, C., Gu, J., Rosenfeld, M. A., Pavan, W. J., Krizman, D. B., Nagle, J., Polymeropoulos, M. H., Sturley, S. L., Ioannou, Y. A., Higgins, M. E., Comly, M., Cooney, A., Brown, A., Kaneski, C. R., Blanchette-Mackie, E. J., Dwyer, N. K., Neufeld, E. B., Chang, T. Y., Liscum, L., Strauss, J. F., Ohno, K., Zeigler, M., Carmi, R., Sokol, J., Markie, D., O'Neill, R. R., van Diggelen, O. P., Elleder, M., Patterson, M. C., Brady, R. O., Vanier, M. T.,

Pentchev, P. G., Tagle, D. A. (1997). Niemann-Pick C1 disease gene: homology to mediators of cholesterol homeostasis. Science *277*, 228-231.

Chen, G., Li, H.M., Chen, Y.R., Gu, X.S., and Duan, S.M. (2007). Decreased estradiol release from astrocytes contributes to the neurodegeneration in a mouse model of Niemann-Pick disease type C. Glia *55*, 1509-1518.

Chen, R., and Ende, N. (2000). The potential for the use of mononuclear cells from human umbilical cord blood in the treatment of amyotrophic lateral sclerosis in SOD1 mice. J Med *31*, 21-30.

Cheng, N., Cai, H.B., and Belluscio, L. (2011). In vivo olfactory model of APP-induced neurodegeneration reveals a reversible cell-autonomous function. J Neurosci *31*, 13699-13704.

Cherry, J.D., Olschowka, J.A., and O'Banion, M.K. (2014). Neuroinflammation and M2 microglia: the good, the bad, and the inflamed. J Neuroinflammation *11*, 98.

Cho, S.R., Kim, Y.R., Kang, H.S., Yim, S.H., Park, C.I., Min, Y.H., Lee, B. H., Shin, J. C., Lim, J. B. (2009). Functional recovery after the transplantation of neurally differentiated mesenchymal stem cells derived from bone barrow in a rat model of spinal cord injury. Cell Transplant *18*, 1359-1368.

Colton, C.A., and Gilbert, D.L. (1987). Production of superoxide anions by a CNS macrophage, the microglia. FEBS letters *223*, 284-288.

Crigler, L., Robey, R.C., Asawachaicharn, A., Gaupp, D., and Phinney, D.G. (2006). Human mesenchymal stem cell subpopulations express a variety of neuro-regulatory molecules and promote neuronal cell survival and neuritogenesis. Exp Neurol *198*, 54-64.

Cunningham, C.L., Martinez-Cerdeno, V., and Noctor, S.C. (2013). Microglia regulate the number of neural precursor cells in the developing cerebral cortex. J Neurosci *33*, 4216-4233.

de Baulny, H.O. (2010). Niemann-Pick type C disease: An early diagnosis for a therapeutic hope. Arch Pediatrie *17*, S39-S40.

de Paula, A.S.A., Malmegrim, K.C., Panepucci, R.A., Brum, D.S., Barreira, A.A., Carlos Dos Santos, A., Araujo, A. G., Covas, D. T., Oliveira, M. C., Moraes, D. A., Pieroni, F., Barros, G. M., Simoes, B. P., Nicholas, R., Burt, R. K., Voltarelli, J. C., Muraro, P. A. (2015). Autologous haematopoietic stem cell transplantation reduces abnormalities in the expression of immune genes in multiple sclerosis. Clin Sci (Lond) *128*, 111-120.

Doty, R.L. (2012). Olfactory dysfunction in Parkinson disease. Nat Rev Neurol *8*, 329-339.

Dziennis, S., and Alkayed, N.J. (2008). Role of signal transducer and activator of transcription 3 in neuronal survival and regeneration. Rev Neurosci *19*, 341-361.

Eckert, M.A., Vu, Q., Xie, K., Yu, J., Liao, W., Cramer, S.C., Zhao, W. (2013). Evidence for high translational potential of mesenchymal stromal cell therapy to improve recovery from ischemic stroke. Journal of cerebral blood flow and metabolism *33*, 1322-1334.

Ekdahl, C.T., Claasen, J.H., Bonde, S., Kokaia, Z., and Lindvall, O. (2003). Inflammation is detrimental for neurogenesis in adult brain. P Natl Acad Sci USA *100*, 13632-13637.

Elrick, M.J., Pacheco, C.D., Yu, T., Dadgar, N., Shakkottai, V.G., Ware, C., Paulson, H. L., Lieberman, A. P. (2010). Conditional Niemann-Pick C mice demonstrate cell autonomous

Purkinje cell neurodegeneration. Human molecular genetics *19*, 837-847.

Ende, N., and Chen, R. (2002). Parkinson's disease mice and human umbilical cord blood. J Med *33*, 173-180.

Ende, N., Weinstein, F., Chen, R., and Ende, M. (2000). Human umbilical cord blood effect on sod mice (amyotrophic lateral sclerosis). Life Sci *67*, 53-59.

Erickson, R.P. (2013). Current controversies in Niemann-Pick C1 disease: steroids or gangliosides; neurons or neurons and glia. J Appl Genet *54*, 215-224.

Fiske, B.K., and Brunjes, P.C. (2000). Microglial activation in the developing rat olfactory bulb. Neuroscience *96*, 807-815.

Fraile, P.Q., Hernandez, E.M., de Aragon, A.M., Macias-Vidal, J., Coll, M.J., Espert, A.N., Silva, M. T. G. (2010). Niemann-Pick type C disease: From neonatal cholestasis to neurological degeneration. Different phenotypes. An Pediatr *73*, 257-263.

German, D.C., Liang, C.L., Song, T., Yazdani, U., Xie, C., and Dietschy, J.M. (2002). Neurodegeneration in the Niemann-Pick C mouse: Glial involvement. Neuroscience *109*, 437-450.

Gheusi, C., Cremer, H., McLean, H., Chazal, G., Vincent, J.D., and Lledo, P.M. (2000). Importance of newly generated neurons in the adult olfactory bulb for odor discrimination. P Natl Acad Sci USA *97*, 1823-1828.

Ginhoux, F., Lim, S., Hoeffel, G., Low, D., and Huber, T. (2013). Origin and differentiation of microglia. Front Cell Neurosci *7*.

Glavaski-Joksimovic, A., Virag, T., Chang, Q.A., West, N.C., Mangatu, T.A., McGrogan, M.P., Dugich-Djordjevic, M., Bohn, M. C. (2009). Reversal of dopaminergic degeneration in a parkinsonian rat following micrografting of human bone marrow-derived neural progenitors. Cell Transplant *18*, 801-814.

Griffin, L.D., Gong, W., Verot, L., and Mellon, S.H. (2004). Niemann-Pick type C disease involves disrupted neurosteroidogenesis and responds to allopregnanolone. Nat Med *10*, 704-711.

Grote, H.E., and Hannan, A.J. (2007). Regulators of adult neurogenesis in the healthy and diseased brain. Clinical and experimental pharmacology & physiology *34*, 533-545.

Hanukoglu, I. (1992). Steroidogenic enzymes: structure, function, and role in regulation of steroid hormone biosynthesis. The Journal of steroid biochemistry and molecular biology *43*, 779-804.

Henderson, L.P., Lin, L., Prasad, A., Paul, C.A., Chang, T.Y., and Maue, R.A. (2000). Embryonic striatal neurons from niemann-pick type C mice exhibit defects in cholesterol metabolism and neurotrophin responsiveness. J Biol Chem *275*, 20179-20187.

Heron, B., and Ogier, H. (2010). Niemann-Pick type C disease: Clinical. presentations in pediatric patients. Arch Pediatrie *17*, S45-S49.

Higashi, Y., Murayama, S., Pentchev, P.G., and Suzuki, K. (1993). Cerebellar Degeneration in the Niemann-Pick Type-C Mouse. Acta Neuropathol *85*, 175-184.

Hovakimyan, M., Meyer, A., Lukas, J., Luo, J.K., Gudziol, V., Hummel, T., Rolfs, A., Wree, A., Witt, M. (2013). Olfactory Deficits in Niemann-Pick Type C1 Disease. Plos One *8*.

Ikonen, E. (2008). Cellular cholesterol trafficking and compartmentalization. Nature reviews Molecular cell biology *9*, 125-138.

Jiang, Y., Jahagirdar, B.N., Reinhardt, R.L., Schwartz, R.E., Keene, C.D., Ortiz-Gonzalez, X.R., Reyes, M., Lenvik, T., Lund, T., Blackstad, M., Du, J., Aldrich, S., Lisberg, A., Low, W. C., Largaespada, D. A., Verfaillie, C. M. (2002). Pluripotency of mesenchymal stem cells derived from adult marrow. Nature *418*, 41-49.

Jin, L.W., Maezawa, I., Vincent, I., and Bird, T. (2004). Intracellular accumulation of amyloidogenic fragments of amyloid-β precursor protein in neurons with Niemann-Pick type C defects is associated with endosomal abnormalities. Am J Pathol *165*, 1447-1447.

Joyce, N., Annett, G., Wirthlin, L., Olson, S., Bauer, G., Nolta, J.A. (2010). Mesenchymal stem cells for the treatment of neurodegenerative disease. Regenerative medicine *5*, 933-946.

Karten, B., Peake, K.B., Vance, J.E. (2009). Mechanisms and consequences of impaired lipid trafficking in Niemann-Pick type C1-deficient mammalian cells. Biochimica et biophysica acta *1791*, 659-670.

Kaytor, M.D., and Orr, H.T. (2002). The GSK3β signaling cascade and neurodegenerative disease. Curr Opin Neurobiol *12*, 275-278.

Kim, S.J., Lee, B.H., Lee, Y.S., Kang, K.S. (2007). Defective cholesterol traffic and neuronal differentiation in neural stem cells of Niemann-Pick type C disease improved by valproic acid, a histone deacetylase inhibitor. Biochem Biophys Res Commun *360*, 593-599.

Kim, S.J., Lim, M.S., Kang, S.K., Lee, Y.S., Kang, K.S. (2008). Impaired functions of

neural stem cells by abnormal nitric oxide-mediated signaling in an in vitro model of Niemann-Pick type C disease. Cell Res *18*, 686-694.

Kim, S.U., Lee, H.J., and Kim, Y.B. (2013). Neural stem cell-based treatment for neurodegenerative diseases. Neuropathology : official journal of the Japanese Society of Neuropathology *33*, 491-504.

Kiyota, T., Okuyama, S., Swan, R.J., Jacobsen, M.T., Gendelman, H.E., and Ikezu, T. (2010). CNS expression of anti-inflammatory cytokine interleukin-4 attenuates Alzheimer's disease-like pathogenesis in APP+PS1 bigenic mice. Faseb J *24*, 3093-3102.

Ko, D.C., Milenkovic, L., Beier, S.M., Manuel, H., Buchanan, J., and Scott, M.P. (2005). Cell-autonomous death of cerebellar Purkinje neurons with autophagy in Niemann-Pick type C disease. PLoS genetics *1*, 81-95.

Kobayashi, T., Beuchat, M.H., Lindsay, M., Frias, S., Palmiter, R.D., Sakuraba, H., Parton, R. G., Gruenberg, J. (1999). Late endosomal membranes rich in lysobisphosphatidic acid regulate cholesterol transport. Nat Cell Biol *1*, 113-118.

Koh, S.H., Kim, K.S., Choi, M.R., Jung, K.H., Park, K.S., Chai, Y.G., Roh, W., Hwang, S. J., Ko, H. J., Huh, Y. M., Kim, H. T., Kim, S. H. (2008). Implantation of human umbilical cord-derived mesenchymal stem cells as a neuroprotective therapy for ischemic stroke in rats. Brain Res *1229*, 233-248.

Komohara, Y., Ohnishi, K., Kuratsu, J., and Takeya, M. (2008). Possible involvement of the M2 anti-inflammatory macrophage phenotype in growth of human gliomas. J Pathol *216*, 15-24.

Kuhn, H.G., Dickinson-Anson, H., and Gage, F.H. (1996). Neurogenesis in the dentate

gyrus of the adult rat: age-related decrease of neuronal progenitor proliferation. J Neurosci *16*, 2027-2033.

Kwon, H.J., Abi-Mosleh, L., Wang, M.L., Deisenhofer, J., Goldstein, J.L., Brown, M.S., Infante, R. E. (2009). Structure of N-terminal domain of NPC1 reveals distinct subdomains for binding and transfer of cholesterol. Cell *137*, 1213-1224.

Lachmann, R.H., te Vruchte, D., Lloyd-Evans, E., Reinkensmeier, G., Sillence, D.J., Fernandez-Guillen, L., Dwek, R. A., Butters, T. D., Cox, T. M., Platt, F. M. (2004). Treatment with miglustat reverses the lipid-trafficking defect in Niemann-Pick disease type C. Neurobiol Dis *16*, 654-658.

Lazarini, F., Gabellec, M.M., Torquet, N., and Lledo, P.M. (2012). Early activation of microglia triggers long-lasting impairment of adult neurogenesis in the olfactory bulb. J Neurosci *32*, 3652-3664.

Lazarini, F., and Lledo, P.M. (2011). Is adult neurogenesis essential for olfaction? Trends Neurosci *34*, 20-30.

Lee, H., Lee, J.K., Min, W.K., Bae, J.H., He, X., Schuchman, E.H., Bae, J. S., Jin, H. K. (2010). Bone marrow-derived mesenchymal stem cells prevent the loss of Niemann-Pick type C mouse Purkinje neurons by correcting sphingolipid metabolism and increasing sphingosine-1-phosphate. Stem Cells *28*, 821-831.

Leung, W., Ramirez, M., Mukherjee, G., Perlman, E.J., and Civin, C.I. (1999). Comparisons of alloreactive potential of clinical hematopoietic grafts. Transplantation *68*, 628-635.

Levitt, P., Harvey, J.A., Friedman, E., Simansky, K., and Murphy, E.H. (1997). New

evidence for neurotransmitter influences on brain development. Trends Neurosci *20*, 269-274.

Lindvall, O., and Kokaia, Z. (2010) Stem cells in human neurodegenerative disorders--time for clinical translation? J Clin Invest *120*, 29-40.

Lindvall, O., Kokaia, Z., and Martinez-Serrano, A. (2004). Stem cell therapy for human neurodegenerative disorders-how to make it work. Nat Med *10 Suppl*, S42-50.

Liu, B., Gao, H.M., Wang, J.Y., Jeohn, G.H., Cooper, C.L., and Hong, J.S. (2002). Role of nitric oxide in inflammation-mediated neurodegeneration. Annals of the New York Academy of Sciences *962*, 318-331.

Liu, B., Xie, C., Richardson, J.A., Turley, S.D., and Dietschy, J.M. (2007). Receptor-mediated and bulk-phase endocytosis cause macrophage and cholesterol accumulation in Niemann-Pick C disease. J Lipid Res *48*, 1710-1723.

Lledo, P.M., Gheusi, G., and Vincent, J.D. (2005). Information processing in the mammalian olfactory system. Physiological reviews *85*, 281-317.

Lledo, P.M., Merkle, F.T., and Alvarez-Buylla, A. (2008). Origin and function of olfactory bulb interneuron diversity. Trends Neurosci *31*, 392-400.

Loftus, S.K., Morris, J.A., Carstea, E.D., Gu, J.Z., Cummings, C., Brown, A., Ellison, J., Ohno, K., Rosenfeld, M. A., Tagle, D. A., Pentchev, P. G., Pavan, W. J. (1997). Murine model of Niemann-Pick C disease: mutation in a cholesterol homeostasis gene. Science *277*, 232-235.

Lopez, M.E., Klein, A.D., Dimbil, U.J., and Scott, M.P. (2011). Anatomically defined

neuron-based rescue of neurodegenerative Niemann-Pick type C disorder. J Neurosci *31*, 4367-4378.

Masliah, E., Alford, M., DeTeresa, R., Mallory, M., and Hansen, L. (1996). Deficient glutamate transport is associated with neurodegeneration in Alzheimer's disease. Ann Neurol *40*, 759-766.

McKeown, D.A., Doty, R.L., Perl, D.P., Frye, R.E., Simms, I., and Mester, A. (1996). Olfactory function in young adolescents with Down's syndrome. J Neurol Neurosur Ps *61*, 412-414.

Meikle, P.J., Hopwood, J.J., Clague, A.E., and Carey, W.F. (1999). Prevalence of lysosomal storage disorders. JAMA *281*, 249-254.

Ming, G.L., and Song, H. (2011). Adult neurogenesis in the mammalian brain: significant answers and significant questions. Neuron *70*, 687-702.

Mosser, D.M., and Edwards, J.P. (2008). Exploring the full spectrum of macrophage activation. Nat Rev Immunol *8*, 958-969.

Mouret, A., Lepousez, G., Gras, J., Gabellec, M.M., and Lledo, P.M. (2009). Turnover of Newborn Olfactory Bulb Neurons Optimizes Olfaction. J Neurosci *29*, 12302-12314.

Murphy, C., Schubert, C.R., Cruickshanks, K.J., Klein, B.E.K., Klein, R., and Nondahl, D.M. (2002). Prevalence of olfactory impairment in older adults. J Am Med Assoc *288*, 2307-2312.

Nakano-Doi, A., Nakagomi, T., Fujikawa, M., Nakagomi, N., Kubo, S., Lu, S., Yoshikawa, H., Soma, T., Taguchi, A., Matsuyama, T. (2010). Bone marrow mononuclear

cells promote proliferation of endogenous neural stem cells through vascular niches after cerebral infarction. Stem Cells *28*, 1292-1302.

Nikolic, W.V., Hou, H., Town, T., Zhu, Y., Giunta, B., Sanberg, C.D., Zeng, J., Luo, D., Ehrhart, J., Mori, T., Sanberg, P. R., Tan, J. (2008). Peripherally administered human umbilical cord blood cells reduce parenchymal and vascular β-amyloid deposits in Alzheimer mice. Stem Cells Dev *17*, 423-439.

Nissant, A., Bardy, C., Katagiri, H., Murray, K., and Lledo, P.M. (2009). Adult neurogenesis promotes synaptic plasticity in the olfactory bulb. Nat Neurosci *12*, 728-730.

Nissant, A., and Pallotto, M. (2011). Integration and maturation of newborn neurons in the adult olfactory bulb - from synapses to function. Eur J Neurosci *33*, 1069-1077.

Ong, W.Y., Kumar, U., Switzer, R.C., Sidhu, A., Suresh, G., Hu, C.Y., Patel, S. C. (2001). Neurodegeneration in Niemann-Pick type C disease mice. Exp Brain Res *141*, 218-231.

Orth, M., and Bellosta, S. (2012). Cholesterol: its regulation and role in central nervous system disorders. Cholesterol *2012*, 292598.

Park, S.B., Yu, K.R., Jung, J.W., Lee, S.R., Roh, K.H., Seo, M.S., Park, J. R., Kang, S. K., Lee, Y. S., Kang, K. S. (2009). bFGF enhances the IGFs-mediated pluripotent and differentiation potentials in multipotent stem cells. Growth Factors *27*, 425-437.

Patterson, M.C., Vecchio, D., Prady, H., Abel, L., and Wraith, J.E. (2007). Miglustat for treatment of Niemann-Pick C disease: a randomised controlled study. Lancet Neurol *6*, 765-772.

Paul, C.A., Boegle, A.K., and Maue, R.A. (2004). Before the loss: neuronal dysfunction

in Niemann-Pick type C disease. BBA-Mol Cell Biol L *1685*, 63-76.

Peake, K.B., Campenot, R.B., Vance, D.E., and Vance, J.E. (2011). Niemann-Pick type C1 deficiency in microglia does not cause neuron death in vitro. BBA-Mol Basis Dis *1812*, 1121-1129.

Peake, K.B., and Vance, J.E. (2010). Defective cholesterol trafficking in Niemann-Pick C-deficient cells. FEBS letters *584*, 2731-2739.

Pentchev, P.G., Comly, M.E., Kruth, H.S., Vanier, M.T., Wenger, D.A., Patel, S., Brady, R. O. (1985). A defect in cholesterol esterification in Niemann-Pick disease type C patients. P Natl Acad Sci USA *82*, 8247-8251.

Perry, V.H., Nicoll, J.A., and Holmes, C. (2010). Microglia in neurodegenerative disease. Nat Rev Neurol *6*, 193-201.

Pfrieger, F.W. (2003). Cholesterol homeostasis and function in neurons of the central nervous system. Cell Mol Life Sci *60*, 1158-1171.

Phinney, D.G., and Prockop, D.J. (2007). Concise review: mesenchymal stem/multipotent stromal cells: the state of transdifferentiation and modes of tissue repair--current views. Stem Cells *25*, 2896-2902.

Pickering, M., Cumiskey, D., and O'Connor, J.J. (2005). Actions of TNF-α on glutamatergic synaptic transmission in the central nervous system. Experimental physiology *90*, 663-670.

Pozharskaya, T., Liang, J., and Lane, A.P. (2013). Regulation of inflammation-associated olfactory neuronal death and regeneration by the type II tumor necrosis factor receptor.

Int Forum Allergy Rh *3*, 740-747.

Prockop, D.J. (2009). Repair of tissues by adult stem/progenitor cells (MSCs): controversies, myths, and changing paradigms. Mol Ther *17*, 939-946.

Puri, V., Watanabe, R., Dominguez, M., Sun, X., Wheatley, C.L., Marks, D.L., Pagano, R. E. (1999). Cholesterol modulates membrane traffic along the endocytic pathway in sphingolipid-storage diseases. Nature cell biology *1*, 386-388.

Ren, G., Zhang, L., Zhao, X., Xu, G., Zhang, Y., Roberts, A.I., Zhao, R. C., Shi, Y. (2008). Mesenchymal stem cell-mediated immunosuppression occurs via concerted action of chemokines and nitric oxide. Cell stem cell *2*, 141-150.

Repa, J.J., Li, H., Frank-Cannon, T.C., Valasek, M.A., Turley, S.D., Tansey, M.G., Dietschy, J. M. (2007). Liver X receptor activation enhances cholesterol loss from the brain, decreases neuroinflammation, and increases survival of the NPC1 mouse. J Neurosci *27*, 14470-14480.

Rimkunas, V.M., Graham, M.J., Crooke, R.M., and Liscum, L. (2009). TNF-α plays a role in hepatocyte apoptosis in Niemann-Pick type C liver disease. J Lipid Res *50*, 327-333.

Rosenbaum, A.I., and Maxfield, F.R. (2011). Niemann-Pick type C disease: molecular mechanisms and potential therapeutic approaches. Journal of neurochemistry *116*, 789-795.

Rosenbaum, A.I., Zhang, G.T., Warren, J.D., and Maxfield, F.R. (2010). Endocytosis of beta-cyclodextrins is responsible for cholesterol reduction in Niemann-Pick type C mutant cells. P Natl Acad Sci USA *107*, 5477-5482.

Sadan, O., Bahat-Stromza, M., Barhum, Y., Levy, Y.S., Pisnevsky, A., Peretz, H., Ilan, A. B., Bulvik, S., Shemesh, N., Krepel, D., Cohen, Y., Melamed, E., Offen, D. (2009). Protective effects of neurotrophic factor-secreting cells in a 6-OHDA rat model of Parkinson disease. Stem cells and development *18*, 1179-1190.

Sarkar, S., Carroll, B., Buganim, Y., Maetzel, D., Ng, A.H., Cassady, J.P., Cohen, M. A., Chakraborty, S., Wang, H., Spooner, E., Ploegh, H., Gsponer, J., Korolchuk, V. I., Jaenisch, R. (2013). Impaired autophagy in the lipid-storage disorder Niemann-Pick type C1 disease. Cell reports *5*, 1302-1315.

Sarna, J.R., Larouche, M., Marzban, H., Sillitoe, R.V., Rancourt, D.E., and Hawkes, R. (2003a). Patterned Purkinje cell degeneration in mouse models of Niemann-Pick type C disease. J Comp Neurol *456*, 279-291.

Sarna, J.R., Larouche, M., Marzban, H., Sillitoe, R.V., Rancourt, D.E., and Hawkes, R. (2003b). Patterned Purkinje cell degeneration in mouse models of Niemann-Pick type C disease. J Comp Neurol *456*, 279-291.

Seo, K.W., Lee, S.R., Bhandari, D.R., Roh, K.H., Park, S.B., So, A.Y., Jung, J. W., Seo, M. S., Kang, S. K., Lee, Y. S., Kang, K. S. (2009). OCT4A contributes to the stemness and multi-potency of human umbilical cord blood-derived multipotent stem cells. Biochem Biophys Res Commun *384*, 120-125.

Seo, Y., Yang, S.R., Jee, M.K., Joo, E.K., Roh, K.H., Seo, M.S., Han, T. H., Lee, S. Y., Ryu, P. D., Jung, J. W., Seo, K. W., Kang, S. K., Kang, K. S. (2011). Human umbilical cord blood-derived mesenchymal stem cells protect against neuronal cell death and ameliorate motor deficits in Niemann Pick type C1 mice. Cell transplantation *20*, 1033-1047.

Shipley, M.T., and Ennis, M. (1996). Functional organization of olfactory system. Journal of neurobiology *30*, 123-176.

Sierra, A., Beccari, S., Diaz-Aparicio, I., Encinas, J.M., Comeau, S., and Tremblay, M.E. (2014). Surveillance, phagocytosis, and inflammation: how never-resting microglia influence adult hippocampal neurogenesis. Neural plasticity *2014*, 610343.

Sierra, A., Encinas, J.M., Deudero, J.J.P., Chancey, J.H., Enikolopov, G., Overstreet-Wadiche, L.S., Tsirka, S. E., Maletic-Savatic, M. (2010). Microglia shape adult hippocampal neurogenesis through apoptosis-coupled phagocytosis. Cell stem cell *7*, 483-495.

Smith, D., Wallom, K.L., Williams, I.M., Jeyakumar, M., and Platt, F.M. (2009). Beneficial effects of anti-inflammatory therapy in a mouse model of Niemann-Pick disease type C1. Neurobiol Dis *36*, 242-251.

Sturley, S.L., Patterson, M.C., Balch, W., and Liscum, L. (2004). The pathophysiology and mechanisms of NP-C disease. Biochim Biophys Acta *1685*, 83-87.

Subramanian, K., and Balch, W.E. (2008). NPC1/NPC2 function as a tag team duo to mobilize cholesterol. P Natl Acad Sci USA *105*, 15223-15224.

Taguchi, A., Soma, T., Tanaka, H., Kanda, T., Nishimura, H., Yoshikawa, H., Tsukamoto, Y., Iso, H., Fujimori, Y., Stern, D. M., Naritomi, H., Matsuyama, T. (2004). Administration of CD34+ cells after stroke enhances neurogenesis via angiogenesis in a mouse model. The Journal of clinical investigation *114*, 330-338.

Tang, Y., Li, H., and Liu, J.P. (2010). Niemann-Pick disease type C: From molecule to clinic. Clin Exp Pharmacol P *37*, 132-140.

Tanna, T., and Sachan, V. (2014). Mesenchymal stem cells: potential in treatment of neurodegenerative diseases. Current stem cell research & therapy *9*, 513-521.

Torrente, Y., and Polli, E. (2008). Mesenchymal stem cell transplantation for neurodegenerative diseases. Cell Transplant *17*, 1103-1113.

Tremblay, M.E., Stevens, B., Sierra, A., Wake, H., Bessis, A., and Nimmerjahn, A. (2011). The role of microglia in the healthy brain. J Neurosci *31*, 16064-16069.

Turner, J.H., Liang, K.L., May, L., and Lane, A.P. (2010). Tumor necrosis factor-α inhibits olfactory regeneration in a transgenic model of chronic rhinosinusitis-associated olfactory loss. Am J Rhinol Allergy *24*, 336-340.

Vance, J.E. (2006). Lipid imbalance in the neurological disorder, Niemann-Pick C disease. FEBS letters *580*, 5518-5524.

Vanier, M.T. (2010). Niemann-Pick disease type C. Orphanet journal of rare diseases *5*, 16.

Vanier, M.T., and Millat, G. (2003). Niemann-Pick disease type C. Clin Genet *64*, 269-281.

Vercelli, A., Mereuta, O.M., Garbossa, D., Muraca, G., Mareschi, K., Rustichelli, D., Ferrero, I., Mazzini, L., Madon, E., Fagioli, F. (2008). Human mesenchymal stem cell transplantation extends survival, improves motor performance and decreases neuroinflammation in mouse model of amyotrophic lateral sclerosis. Neurobiol Dis *31*, 395-405.

von Bernhardi, R., and Eugenin, J. (2004). Microglial reactivity to β-amyloid is

modulated by astrocytes and proinflammatory factors. Brain research *1025*, 186-193.

Vukovic, J., Colditz, M.J., Blackmore, D.G., Ruitenberg, M.J., and Bartlett, P.F. (2012). Microglia modulate hippocampal neural precursor activity in response to exercise and aging. J Neurosci *32*, 6435-6443.

Walkley, S., Davidson, C., Ali, N., and Vanier, M. (2010). Cyclodextrin treatment not only delays but also reduces established intraneuronal storage in Niemann-Pick type C disease. Mol Genet Metab *99*, S37-S37.

Walter, J., Keiner, S., Witte, O.W., and Redecker, C. (2011). Age-related effects on hippocampal precursor cell subpopulations and neurogenesis. Neurobiol Aging *32*, 1906-1914.

Wilson, R.S., Arnold, S.E., Schneider, J.A., Boyle, P.A., Buchman, A.S., and Bennett, D.A. (2009). Olfactory impairment in presymptomatic Alzheimer's disease. Ann Ny Acad Sci *1170*, 730-735.

Winner, B., Kohl, Z., and Gage, F.H. (2011). Neurodegenerative disease and adult neurogenesis. Eur J Neurosci *33*, 1139-1151.

Wraith, J.E., Vecchio, D., Jacklin, E., Abel, L., Chadha-Boreham, H., Luzy, C., Giorgino, R., Patterson, M. C. (2010). Miglustat in adult and juvenile patients with Niemann Pick disease type C: Long-term data from a clinical trial. Mol Genet Metab *99*, 351-357.

Wu, Y.P., Mizukami, H., Matsuda, J., Saito, Y., Proia, R.L., and Suzuki, K. (2005). Apoptosis accompanied by up-regulation of TNF-α death pathway genes in the brain of Niemann-Pick type C disease. Mol Genet Metab *84*, 9-17.

Xu, S., Benoff, B., Liou, H.L., Lobel, P., and Stock, A.M. (2007). Structural basis of sterol binding by NPC2, a lysosomal protein deficient in Niemann-Pick type C2 disease. J Biol Chem *282*, 23525-23531.

Yang, M., and Crawley, J.N. (2009). Simple behavioral assessment of mouse olfaction. Current protocols in neuroscience *Chapter 8*, Unit 8.24.

Yang, S.R., Kim, S.J., Byun, K.H., Hutchinson, B., Lee, B.H., Michikawa, M., Lee, Y. S., Kang, K. S. (2006). NPC1 gene deficiency leads to lack of neural stem cell self-renewal and abnormal differentiation through activation of p38 mitogen-activated protein kinase signaling. Stem Cells *24*, 292-298.

Ye, J., and DeBose-Boyd, R.A. (2011). Regulation of cholesterol and fatty acid synthesis. Cold Spring Harbor perspectives in biology *3*.

Yu, T., and Lieberman, A.P. (2013). Npc1 acting in neurons and glia is essential for the formation and maintenance of CNS myelin. PLoS genetics *9*.

Yu, T., Shakkottai, V.G., Chung, C., and Lieberman, A.P. (2011). Temporal and cell-specific deletion establishes that neuronal Npc1 deficiency is sufficient to mediate neurodegeneration. Human molecular genetics *20*, 4440-4451.

Zhao, C.P., Zhang, C., Zhou, S.N., Xie, Y.M., Wang, Y.H., Huang, H., Shang, Y. C., Li, W. Y., Zhou, C., Yu, M. J., Feng, S. W. (2007). Human mesenchymal stromal cells ameliorate the phenotype of SOD1-G93A ALS mice. Cytotherapy *9*, 414-426.

국문 초록

니만-픽크 C1 형 질환에서

신경 퇴행성 변화의 완화 기전

서울대학교 대학원

수의학과 수의공중보건학 전공

서 유 진

(지도교수: 강경선)

니만-픽크 C형 질환은 콜레스테롤 대사에 관여하는 니만-픽크 C 단백질의 기능이상에 의해 발병하는 지질대사 장애로 대부분의 환자가 20대에 이르기 전에 사망하는 불치성 신경퇴행성 질환이다. 신경증상이 발현하는 시기와 환자

의 예후 간에 밀접한 연관이 있음이 밝혀짐에 따라 신경 손상의 기전을 이해하는 것이 니만-픽크 C형 질환의 치료법을 개발하는 데 필수적이라는 의견이 대두되고 있으며, 본 연구 또한 여기에 주안점을 두고 니만-픽크 C1형 질환 모델 마우스의 신경성 병변을 완화시키는 새로운 방법을 모색하고자 하였다.

첫 번째 연구는 사람 제대혈 유래 중간엽 줄기세포가 니만-픽크 C1형 질환의 신경증상 개선을 위한 긍정적인 역할을 수행할 것이라는 가설을 바탕으로 진행되었다. 이 가설을 증명하기 위해, 사람 제대혈 유래 중간엽 줄기세포를 니만-픽크 C1형 질환 모델 마우스의 해마에 직접 주입한 뒤 그 효과를 평가하였다. 세포 투여의 결과 질환 마우스의 운동기능이 향상되었고 콜레스테롤 배출 기능이 활성화 되어 세포 내 콜레스테롤 침착 량이 감소하였다. 또한 사람 제대혈 유래 중간엽 줄기세포의 투여는 해마를 구성하는 신경세포의 생존율 및 신경줄기세포의 증식을 증가시켰으며, 주입된 세포 중 일부는 전기생리학적인 활성을 띄는 신경세포로 직접 분화되는 것을 확인할 수 있었다. 한편 사람 제대혈 유래 중간엽 줄기세포에 의한 염증억제 작용 및 세포사 억제 작용에 의해 세포가 직접 투여된 해마에서뿐만 아니라 니만-픽크 C1형 질환에서 특이적으로 관찰되는 소뇌 조롱박세포 신경세포사의 억제도 관찰되었다. 이러한 신경보호 효과는 세포 생존을 조절하는 신호체계에 속하는 phosphoinositide 3 kinase/AKT (PI3K/AKT) 경로와 Janus kinase 2/signal transducers and activators of transcription protein3 (JAK2/STAT3) 경로의 활성

화에 기인한 것으로 보인다. 또한 니만-픽크 C1형 질환 모델 마우스의 뇌에서는 억제성 신경전달물질인 가바(GABA)와 흥분성 신경전달물질인 글루타메이트(glutamate) 농도 간 불균형으로 인해 흥분성 신경독성이 증가함이 보고되어 있는데, 인간 제대혈 유래 중간엽 줄기세포를 주입한 뒤 가바와 관련된 신경전달물질 운반에 관여하는 유전자들의 발현이 신경독성을 감소시키는 방향으로 조절되는 것이 확인되었다.

또한, 본 연구에서는 신경퇴행성 장애의 진행 초기에 후각의 상실이 나타난다는 점에 착안하여, 니만-픽크 C형 질환에 의해 유도되는 후각 망울의 기능 변화에 대한 연구를 진행하였다. 숨겨진 음식 찾기 시험 법을 이용하여 실험 모델 마우스들의 후각 능력을 평가해본 결과, 7주령의 니만-픽크 C1형 모델 마우스들은 동일한 나이의 정상 마우스에 비해서 현격한 후각기능의 손실이 있음을 알 수 있었다. 조직학적으로 볼 때, 니만-픽크 C1형 모델 마우스의 후각상피 내의 후각표지단백질에 면역반응을 나타내는 세포 수는 현저하게 감소한 것을 확인할 수 있었다. 또한 후각 기능과 관련이 있다고 알려진 뇌실 밑 영역에 존재하는 신경줄기세포들의 증식 정도는 정상 마우스와 아무런 차이가 없음에도 불구하고 후각 망울에 존재하는 신경모세포의 총량은 크게 줄어든 것이 관찰되었다. 또한 니만-픽크 C1형 질환의 신경증상이 진행됨에 따라 후각 망울 내에서는 염증성 미세아교세포의 증식과 축적이 증가함을 확인할 수 있었다. 이에 광범위 항 염증 억제제 중 하나인 사이클로스포린 에이

(Cyclosporin A) 를 4주령의 니만-픽크 C1형 모델 마우스에게 4주간 투여하여 미세아교세포를 불활성화 시켜, 미세아교세포의 활성화와 후각능력의 연관성을 평가하였다. 그 결과, 사이클로스포린 에이의 처치는 니만-픽크 C1형 질환 모델 마우스에서 관찰되던 미세아교세포의 증식을 효과적으로 감소시켰고 새롭게 생성된 신경세포들의 생존을 증가시켰으며 후각기능의 전반적인 향상을 가져왔다.

따라서 본 연구는 니만-픽크 C1형 질환의 여러 신경퇴행성 증상들을 완화시키기 위해 인간 제대혈 유래 중간엽 줄기세포의 주입과 미세아교세포의 억제제의 활용 가능성을 제시함으로써 니만-픽크 C1형 질환 치료 분야에 기여할 수 있을 것으로 기대된다.

주요어 : 니만-픽크 C1 형 질환, 신경퇴행, 인간 제대혈 유래 중간엽 줄기세포, 후각기능, 미세아교세포, 사이클로스포린 에이

학 번 : 2009-21625